Catena 199 (2021) 105087

Contents lists available at ScienceDirect

Catena

journal homepage: www.elsevier.com/locate/catena

# Late Pleistocene paleosol formation in a dynamic aggradational microenvironment - A case study from the Malá nad Hronom loess succession (Slovakia)

B. Bradák [a,*], D. Csonka [b], Á. Novothny [b,c], J. Szeberényi [d], A. Medveďová [e], P. Rostinsky [f], K. Fehér [g], G. Barta [b], T. Végh [b], K. Kiss [b], M. Megyeri [b]

[a] Department of Physics, University of Burgos, Av. de Cantabria, s/n 09006, Burgos, Spain
[b] ELTE Eötvös Loránd University, Institute of Geography and Earth Sciences, Department of Physical Geography, Pázmány Péter sétány 1/C. H-1117, Budapest, Hungary
[c] Leibniz Institute for Applied Geophysics (LIAG), Stilleweg 2, 30655 Hannover, Germany
[d] Geographical Institute, Research Centre for Astronomy and Earth Sciences, 45 Budaörsi út, H-1112 Budapest, Hungary
[e] University of Matej Bel Faculty of Natural Sciences, Banská Bystrica, Tajovského 40, 974 01, Slovak Republic
[f] The Czech Academy of Sciences, Institute of Geonics, Department of Environmental Geography, Drobného 28, 60200 Brno, Czech Republic
[g] ELTE Eötvös Loránd University, Institute of Geography and Earth Sciences, Department of Environmental and Landscape Geography, Pázmány Péter sétány 1/C, H-1117 Budapest, Hungary

ARTICLE INFO

*Keywords:*
Sedimentation
Pedogenesis
Paleogeomorphology
Multiproxy
Heatmap
Principal component analysis

ABSTRACT

The geomorphological characteristics of the loess succession at Malá nad Hronom (Slovakia) mean that it provides a valuable opportunity for the investigation of differences in soil formation in various topographic positions. Along with the semiquantitative characterization of the paleosols (on the basis of physical properties, texture, the characteristics of peds, clay films, horizon boundaries), high-resolution field magnetic susceptibility measurements and sampling were carried out along four different sections of the profile. Samples for luminescence dating were also taken, in order to establish the chronostratigraphical position of the paleosols studied. The comparison of various proxies revealed the differences in soil formation in a dynamic aggradational microenvironment for the same paleosol horizons located in various positions along the slope. Contrary to expectation, paleosols developed in local top or slope topographical positions did not display significant differences in e.g. in their degree of development, nor the characteristics of their magnetic susceptibility curves. In the case of paleosols in positions lower down the slope, signs of quasi-permanent sediment input could be recognized as being present as early as during the formation of the soil itself. This sediment input would seem to be surpassed in the case of pedogenesis strengthened by the climate of the last interglacial (marine isotope stage - MIS 5). Pedogenesis seems to be sustained by renewed intense dust accumulation in the Late Pleistocene, in MIS 3, though compared to MIS 5, the climate of MIS 3 did not favor intense pedogenesis. Despite the general belief that loess series formed in plateau positions can preserve terrestrial records without significant erosion, in the case of the Malá nad Hronom loess this is not so. Compared to the sequence affected by erosional events in the local top position, the sequence affected by quasi-continuous sediment input in the lower slope position seems to have preserved the soil horizons intact.

## 1. Introduction

There are many applications of paleosol horizons in geology. For example, paleosols can be used in stratigraphic studies as marker horizons for the local and regional correlations; they can be used to interpret and reconstruct paleogeomorphology via the analysis of paleosol–landscape associations; and paleosols are also helpful in the reconstruction of paleoclimate (Kraus, 1999).

On the local scale, lateral changes in the characteristics of paleosols formed on clastic sediments reflect the grain size of the parent material and, indirectly, the geomorphology (topography). At the regional level – so, say, in the case of a sedimentary basin – paleosol properties reflect

* Corresponding author.
*E-mail address:* b.bradak-hayashi@ubu.es (B. Bradák).

https://doi.org/10.1016/j.catena.2020.105087
Received 12 June 2020; Received in revised form 23 November 2020; Accepted 28 November 2020
Available online 19 December 2020

local differences in clastic sedimentary characteristics (grain size), topography, climate and subsidence/accumulation rates (Kraus, 1999).

A vast amount of knowledge concerning paleosol horizons and their significance in the reconstruction of interglacial climate is available – for useful summaries of paleosols in loess, see e.g. in Muhs and Bettis (2003) and Mush (2007a, b). Here the focus is on those studies, considerably fewer in number, which go beyond this, attempting to map the influence of paleogeomorphological variation and the differences in sedimentation rate (i.e. the local variation of paleosol horizons) in the development of what are considered to be the same paleosol units in loess-paleosol sequences.

Although most studies of loess-paleosol sequences focus on so-called plateau loess (e.g. Marković et al., 2015), in which the likelihood of erosional hiatuses and redeposition is minimal, research revealing the potential of non-plateau loess in complex environment reconstructions does exist – it should be noted that here, 'non-plateau' refers to any type of loess succession formed in non-plateau paleotopographical position, such as Veröce, Hévízgyörk, and Süttő (see below).

On the basis of the characterization of a loess-paleosol sequence formed on a paleoslope, Bradák et al. (2011) and Bradák-Hayashi et al. (2016) were able to describe complete climate cycles. The model presented involved redeposited loess horizons as a marker of the transition environment between pedogenic (interglacial) and sedimentary (glacial) phases. The studies also used the redeposited loess to characterize the paleoenvironment of such transition periods.

One of the most complex studies of loess profiles influenced by slope processes was conducted on the Late Pleistocene Krems-Wachtberg succession (e.g. Händel et al., 2009a, b; Hambach, 2010; Terhorst et al., 2014). The Krems-Wachtberg loess succession is famous for a complex formation influenced in particular but not exclusively by slope processes: besides the dominant aeolian activity and stable and short periods of pedogenesis, erosional processes contributed to the forming of the sequence, while in the course of the reduced phases of aeolian sedimentation, the formation of Cryosols and permafrost processes became dominant. What is more, some parts of the sequence were affected by solifluction and erosional processes on slope (for a summary, see Terhorst et al., 2014). However, in the case of the Krems-Wachtberg loess succession, "there is evidence that erosional phases/events were not so strong or prolonged, because the sequence reveals a fast sedimentation" (Terhorst et al., 2014, p. 81).

Further studies of Austrian loess from MIS 3-2 demonstrate that "geomorphodynamic processes" (erosion and colluvial processes) exercised a significant influence on the character of sedimentation and polygenetic paleosol formation in those profiles (Terhorst et al., 2015).

The superposition of paleosols in paleoslope positions has been noted in the Hévízgyörk profile (Hungary), as well (Csonka et al., 2020). In this case, the erosional periods and the intermittent nature of the dust accumulation and pedogenic periods caused significant hiatuses in the record, in contrast to the Krems-Wachtberg loess.

In some cases, the influence of paleotopography on soil development can be clearly identified in the loess profiles. Paleosols appear as a paleovalley infill in Süttő (Hungary) (Novothny et al., 2009); the buried reddish-brown, clayey soil horizon does not appear as a continuous horizon in other parts of this outcrop, though it can also be found in the lower part of the quarry, in a (paleo)slope position. In the case of the Süttő sequence, the paleosol complex found in the paleovalley represents a soil complex which had not been observed previously in Hungarian loess profiles. The remains of the same soil horizon found in a paleoslope position, together with and the absolute age results, suggest that intense erosion during the last interglacial (MIS 5) might have played a significant role in the disappearance of the soil horizon.

In another case similar to the Süttő profile, a well-developed paleosol, appearing as a paleovalley infill, was identified in the abandoned brickyard of Verőce (Hungary) (Bradák et al., 2014). Further examination of the profile identified two similar paleosol horizons in slope and local top topographic positions. The absolute age dating of the succession verified that the soil horizons represent the same warm, humid period, namely, the MIS 5 interglacial; this, in turn, provided a unique opportunity for the comparison of the characteristics of pedogenesis from the same paleoclimatic period, but in different paleogeomorphic positions.

Ghafarpour et al. (2016) studied the Mobarakabad and Aghband loess (Iran). In the Mobarakabad succession "the pedocomplex sequence splits into five different paleosols that are intercalated in the loess with anticlinal shapes" (Ghafarpour et al., 2016, p. 97). The relation of paleosol horizons may suggest the influence of tectonic activity (e.g. Machette, 1978), but since no tectonic activity is to be expected in the area (Ghafarpour et al., 2016, referring to Kehl et al., 2005), the anticlinal shape of the loess-paleosol sequence was interpreted as the result of the mantling of a pre-existing land surface (Ghafarpour et al., 2016). The influence of tectonic processes may well require reconsideration following the study by Motavalli-Anbaran et al. (2011), which suggests tectonic activity in the region (in the Alborz Mountains): as indicated by various (magnetic) proxies, the different slope position in the Iranian successions in those studies might cause different levels of exposure to climatic components (e.g. precipitation) during the forming of paleosols (Ghafarpour et al., 2016). In a precursor to the Iranian loess studies, Kehl et al. (2005) had studied and characterized paleosols and soil forming environments in the Basin of Persepolis via the study of sequences consisting of loess, loess-like sediments (redeposited loess) and paleosol horizons in various stages of development.

The above examples show how variable the characteristic of the development of a loess succession in a non-plateau position can be. Although the application of such successions as a key profile in stratigraphic correlation can be called into question due to the possible hiatuses (Marković et al., 2015), they may play a significant role in the description of paleoenvironments. Along with various methods (e.g. micromorphology), the study of the relationship between sedimentation and pedogenesis may provide essential information about the environment in which the soil was formed. Due to the paleotopographical characteristics of the Malá nad Hronom loess profile (a succession developed on a paleoslope; Szeberényi et al., 2020), the study of paleosols may provide a valuable opportunity for the description of the processes of soil formation in aggradational (micro)environments (suggested by Kraus, 1999 and references therein).

The goal of the present study is to characterize the relationship between sedimentation and pedogenesis during soil formation in paleosols in similar chronostratigraphic positions, but in paleo-topographic positions which are varied, and from this to elaborate a model of soil formation from loess in a dynamic aggradational environment. It may help to understand and provide significant information about soil development in "non-ideal" conditions, in which there is interference from erosion and/or quasi-permanent sediment accumulation (e.g. soil formation on a slope instead of on a plateau). Knowledge of soil development on slopes may then be applied to paleosol horizons developed in other non-plateau positions.

## 2. Site and sampling

### 2.1. Geological and geomorphological characteristics of the vicinity of Malá nad Hronom section

The abandoned brickyard is located on the western side of a dissected fluvial terrace of the River Hron, one of the tributaries of River Danube in the vicinity of Malá nad Hronom (130–155 m.a.s.l.; N47°49′46.0″, E19°02′ 33.6″, Slovakia) (Fig. 1a and b).

The lowland Danube Basin (or Danube Lowland) represents a depositional area filled in with various marine, brackish, limnic and fluvial sedimentary sequences of Miocene, Pliocene and Quaternary age (Kováč, 2000; Vass, 2002). Among the pronounced landforms of the easternmost part of the Danube Lowland, Bajtava Gate is a subhorizontal plateau, a remnant of the Middle-Pleistocene fluvial terrace of the Hron

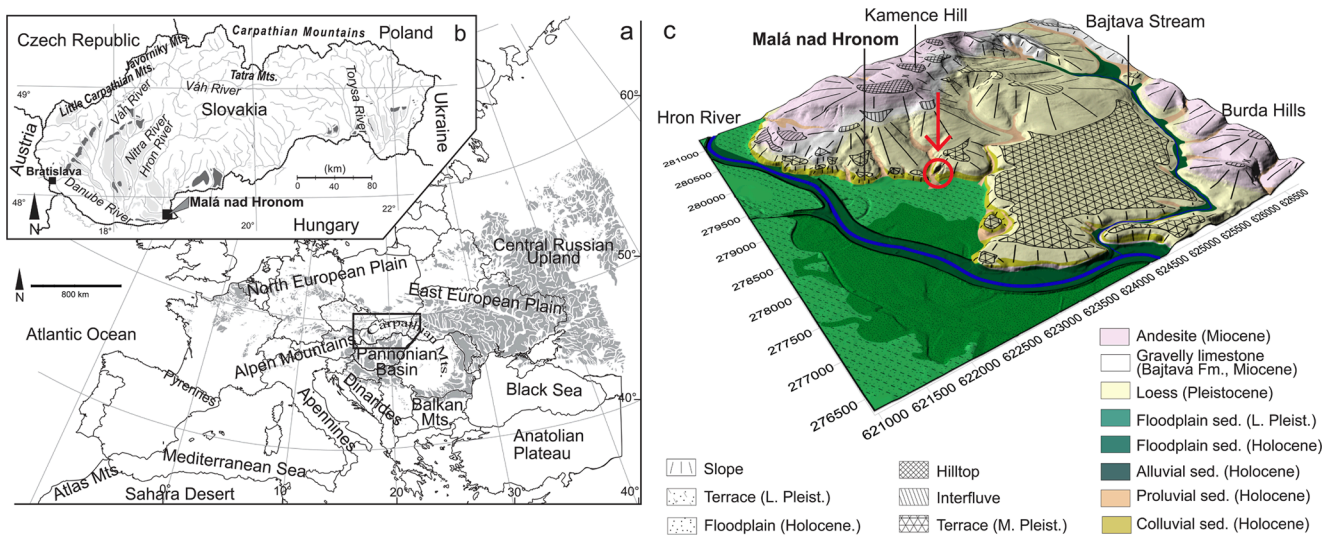


**Fig. 1.** Location of the Malá nad Hronom loess outcrop (a, b), and the basic geological and geomorphological features of its surroundings (c). Fig. 1a and b are after Szeberényi et al. (2020). The digital elevation model was developed using Surfer 8 software (Golden Software) based on the digital geological map (at scale 1:50 000; https://apl.geology.sk/gm50js/) and the digital topological map (at scale 1:10 000; https://zbgis.skgeodesy.sk) of the Slovak Republic. The red arrow with the circle indicates the location of the loess profile studied here. (For interpretation of the references to color in this figure legend, the reader is referred to the web version of this article.)

at the SE edge of the Danubian Hills. The eroded fluvial terrace is covered by loess to a thickness of more than 20 m, in some locations sharply rising ~40 m above the present day river floodplain. The loess plateau extends eastwards and reaches the foothills of the North Hungarian Mountains (Halouzka, 1966; Minaříková, 1969; Mazúrová, 1978) (Fig. 1b and c).

The Malá nad Hronom loess profile is located on the erosionally dissected slope of the plateau, within the Bajtava Gate (between the Burda Hills and Kamence Hill) descending from the top of the plateau surface (the Ipeľská Pahorkatina upland, elevation interval ~270–150 m a.s.l., mean inclination ~5°) (Fig. 1c). In the lowermost part of the slope of the plateau, the gentler slope abruptly turns into a small steep scarp formed by the lateral erosion of the Hron (~150–120 m, mean inclination ~18°). The upper section of the slope is composed of a near-shore geological facies of the so-called Bajtava Formation (Fm). The Bajtava Fm is a basal Miocene (Lower/Middle Badenian) marine sedimentary sequence of the Danube Lowland. Generally, it is represented by coarse transgressive breccia, conglomerates and sandstones with a higher content of andesite volcaniclastics, all being firmly cemented by $CaCO_3$ (Seneš et al., 1970; Vass 2002). In the studied site, this formation appears in the form of grain-supported, gravelly limestone conglomerate rocks including well-sorted, fine-grained pebbles (Szeberényi et al., 2015) (Fig. 1c). Weathered, redeposited debris from the Bajtava Fm. forms a significant component of extensive Quaternary colluvial regolith on the lowermost parts of the gentle slope segment. This colluvial sediment can be found in the (topographically) lowermost part of the outcrop at Malá nad Hronom, along with loess, in the upper section of the abandoned brickyard (Fig. 1c).

## 3. Methods

### 3.1. Proxies used in relation to sedimentary and pedogenic environment

In the course of the field description of paleosols, the method of semiquantitative analysis introduced by Harden (1982) was employed to determine the degree of soil development. On the basis of this, soils can be described using basic properties such as color on the Munsell scale, texture, both dry and moist, appearance of clay films, boundaries between the pedogenic horizons, and the characteristics of peds (aggregates of soil particles). For each soil horizon, points are assigned according to the amount of change in a given soil property relative to its original state in the parent material. Following the normalization of the various points, the horizon index (HI), that is, the sum of points after normalization divided by the number of properties, can be calculated. The results of each horizon are summed along the profile to obtain the profile development index (PDI) (i.e. the degree of development of the soil profile) (Harden, 1982). Besides its application to, for example, the estimation of the duration of soil formation, the Harden index can be used to compare the degree of development of a paleosol in various geomorphological positions (as seen in, for example, Bradák et al., 2014). (Raw and calculated data for HI and PDI indices can be found in Suppl. Mat. 1).

The low field magnetic susceptibility (κlf) measurement was made on the cleaned surface of the profile using a Kappameter KT-5 portable field susceptibility meter (Geofyzika Brno, now ZH Instruments, Czech Republic). The measurement interval was 5 cm, which in practical terms provided a quasi-continuous record. In every 5 cm, 3–5 measurements were carried out and the average of the results was calculated. The average κlf of two measured horizons (i.e. every 10 cm) was then used in the mathematical-statistical comparison of the proxies.

Field κlf measurement is able to characterize and compare the ratio of the bulk magnetic mineral components rapidly, including ferro, para and diamagnetic components, and their vertical change in the succession under examination. In general, loesses from the European Loess Belt (ELB) are characterized by low κlf, whereas paleosols are characterized by high κlf (Marković et al., 2015 and references therein). The differences between the κlf of loess and paleosols can be described in terms of the different amount of authigenic pedogenic magnetic contributors. The magnetic enhancement of loess by pedogenic processes, such as the production of ultrafine (of the order of nanometers) magnetic components e.g. magnetite, by biogenic activity and the formation of maghemite or hematite by various weathering processes has been described in various studies (e.g. Heller et al., 1993; Evans and Heller, 1994; Maher et al., 1994, 2002, 2003; Geiss and Zanner, 2007; Geiss et al., 2008; Balsam et al., 2011; Long et al., 2016) and it is known as the pedogenic enhancement model (e.g. Evans, 2001). Therefore, κlf was employed in this study to identify pedogenic activity and pedogenic horizons as well as in the role of an indicator of the degree of pedogenesis. Nevertheless, this method has its own limitations. As mentioned above, the measurements indicate the relative, "bulk" amount of any magnetic

contributors, but the type of magnetic minerals cannot be detected in the field examination.

The grain size distribution of samples taken from every 10 cm of the studied successions was measured using a Horiba Partica LA 950V2 laser diffraction particle size analyzer (Laser Diffraction Particle Size Distribution Analyzer Laboratory, Eötvös University, Hungary). Before the analyses, samples were treated with 30% hydrogen peroxide ($H_2O_2$), and the carbonate content was removed with the use of a 10% solution of hydrogen chloride (HCl). Grain size classes were assigned in accordance with Konert and Vandenberghe (1997), as follows sand content (>63 μm), coarse sand content (>160 μm) and clay content (<5.5 μm).

Along with the various sediment classes, used mainly during the mathematical-statistical analysis, the U-ratio (the ratio of coarse silt to fine silt: 16–44 μm/5.5–16 μm) was applied as a proxy for changing sedimentary environments. As suggested by Vandenberghe et al. (1997), the clay fraction was disregarded to avoid any influences from authigenic clay formation in soils. The U-ratio can therefore be used as a general proxy for changing sedimentary environments. An increasing U-ratio indicates an increasing coarser silt component and sedimentation (e.g. during glacial periods); in contrast, a lower U-ratio is characteristic of pedogenic (interglacial) periods (Vandenberghe et al., 1997).

The bulk calcium carbonate content was measured at a vertical resolution of 10 cm (78 samples) using a Scheibler calcimeter (Laboratory for sediment and soil analysis, Geographical Institute, Research Centre for Astronomy and Earth Sciences, Budapest, Hungary) and approximately 1 g of material. The mass-specific calcium carbonate content ($CaCO_3$ in g/kg) was calculated with respect to air temperature and pressure. $CaCO_3$ content was used as an indicator of vertical (hydrological) processes in the body of the paleosols such as leaching and precipitation (Shaetzl and Anderson, 2005), and as an important indicator of (vertical) water migration depth in the profile (e.g. Zhao et al., 2020 and the references therein).

### 3.2. Statistical methods

A heatmap is a correlation matrix combined with a color code indicating the strength of the statistical relationships between variables. The heatmap shows the Pearson`s correlation coefficient (r) between the variables under investigation. In this study, r was interpreted in the following way. If r = (-)1, there is a perfect positive or negative linear relationship between the two variables under investigation. A strong positive or negative linear relationship is indicated by r = (-)0.99–0.7. When r = (-)0.69–0.5, the statistical relationship between the two variables is moderate. In the case of r = (-)0.49–0.3, there is a weak uphill or downhill relationship between the variables. And if r falls into the range between −0.29 and 0.29, the statistical relationship between the two variables is insignificant.

Principal component analysis (PCA), a multivariate method, was employed to reduce the dimensionality of a data set consisting of a large number of interrelated variables (here κlf, $CaCO_3$ and grain size information, Suppl. Mat. 1), while retaining as much as possible of the variation present in the data set (Jolliffe, 2002). The reduction is achieved by transforming the data set into a new set with fewer variables (the so-called principal components) using orthogonal transformation. These new variables correspond to a linear combination of the originals. In other words, PCA reduces the dimensionality of multivariate data to two principal components (PCs) with minimal loss of information. The principal components may be supposed to preserve the essential part of data in which more variation is present and remove the data with fewer variations.

Along the PC1 - PC2 plot, the results of PCA can be characterized by the explained variance, explained variance ratios and their sum. Explained variance is used to measure the discrepancy between the actual data and the model (here PC1 and PC2). Higher percentages of explained variance indicate a stronger strength of association (Rosenthal and Rosenthal, 2011). In the case of PCA, the amount of data preserved during the reduction of the dimensionality of multivariate data can be shown by the "explained variance ratio" and "sum of explained variance ratio". In addition, the analysis of "loadings" provides information about the contribution of original variables (e.g. κlf, $CaCO_3$ and grain size information; Suppl. Mat. 1) in PC1 and PC2.

All the statistical analysis was done using the Matplotlib, Numpy, Pandas, Sckit-learn and Seaborn modules of Python (https://www.python.org/).

### 3.3. Luminescence dating method

Optically Stimulated Luminescence (OSL) is a trapped charge dating method suitable for dating young Quaternary sediments. Luminescence dating is able to determine the burial age of the samples, chiefly by measuring the quartz and feldspar in the samples. The age limit that can be determined for feldspar is higher (~200–250 ka) than that of quartz (~100 ka for Hungarian loess sediments), although the Infrared Stimulated Luminescence (IRSL) signal of feldspar can be affected by anomalous fading (Wintle, 1973), which results in the underestimation of age. The post-Infrared Infrared Stimulated Luminescence (pIRIR) method (Buylaert et al., 2009; Thiel et al., 2011) was therefore used in this study to determine the equivalent dose (De) of the samples, as it is not to any great extent affected by fading and its age limit is higher than that of the standard IRSL protocol. Five samples were collected from the cleaned loess wall of the MnH1 and MnH3 successions (Fig. 2b) to determine their luminescence age. Their exact position is shown in Fig. 2.

The polymineral fine-grain fraction (4–11 μm) was prepared for the samples. All samples were treated using 0.1 N hydrochloric acid, 0.01 N sodium-oxalate and 30% hydrogen peroxide to remove carbonate, clay coating and organic matter, respectively, from the samples. All preparations were conducted under subdued red light.

All luminescence measurements were carried out at the luminescence laboratory of the Research and Instrument Core Facility at the Eötvös Loránd University (Budapest, Hungary), using an automated Risø TL/OSL-DA-20 reader. IRSL stimulations were performed for 200 s first at 50 °C and subsequently at 290 °C. The $D_e$ value of the samples was obtained by integrating the initial 2.5 s region of the pIRIR@290 decay curves and subtracting the background, the final 50 s of the stimulation. A single saturation exponential function was fitted to the dose points to obtain the $D_e$ of the aliquots (Suppl. Mat. 2a) and the mean of the $D_e$ values was calculated for the age determination.

Preheating at 320 °C for 60 s was done before the IR stimulations. An extra illumination step (IRSL stimulation at 325 °C for 100 s) was used to reduce recuperation (Murray and Wintle, 2003). For all samples and aliquots recycling was within 5% of unity, and recuperation below 2%.

As the pIRIR@290 signal bleaches more slowly than the OSL signal of quartz and the IR-50 signal of feldspar, a residual test was performed to assess the amount of the residual dose after bleaching. After a three-day daylight bleach, the aliquots were measured using the same protocol. The observed residual dose ranged between 9.9 ± 0.5 Gy (SK-MNH-3) and 23.1 ± 2.1 Gy (SK-MNH-2) and increased with the De of the sample, as shown in Suppl. Mat. 2b. Similar observations have been reported by Buylaert et al. (2012), Yi et al. (2016) and Novothny et al. (2019), and the value of the interception (7.25 Gy) of the fitted linear function was therefore subtracted as a residual dose from each the $D_e$-value for the age calculation, as suggested by Buylaert et al. (2012).

Dose rates were obtained from the potassium, uranium and thorium content, as measured by gamma spectrometry in the laboratory at the Leibniz Institute for Applied Geophysics, in Hannover. These samples were collected from the surroundings of the luminescence sampling tubes, dried at 50 °C in the laboratory, then homogenized and packed into Marinelli containers for gamma spectrometry measurements. The prepared samples were sealed and stored for one month to avoid radioactive disequilibrium between the $^{222}Rn$ and $^{226}Ra$ isotopes. In the present study, the dose rate conversion is based upon the factors of

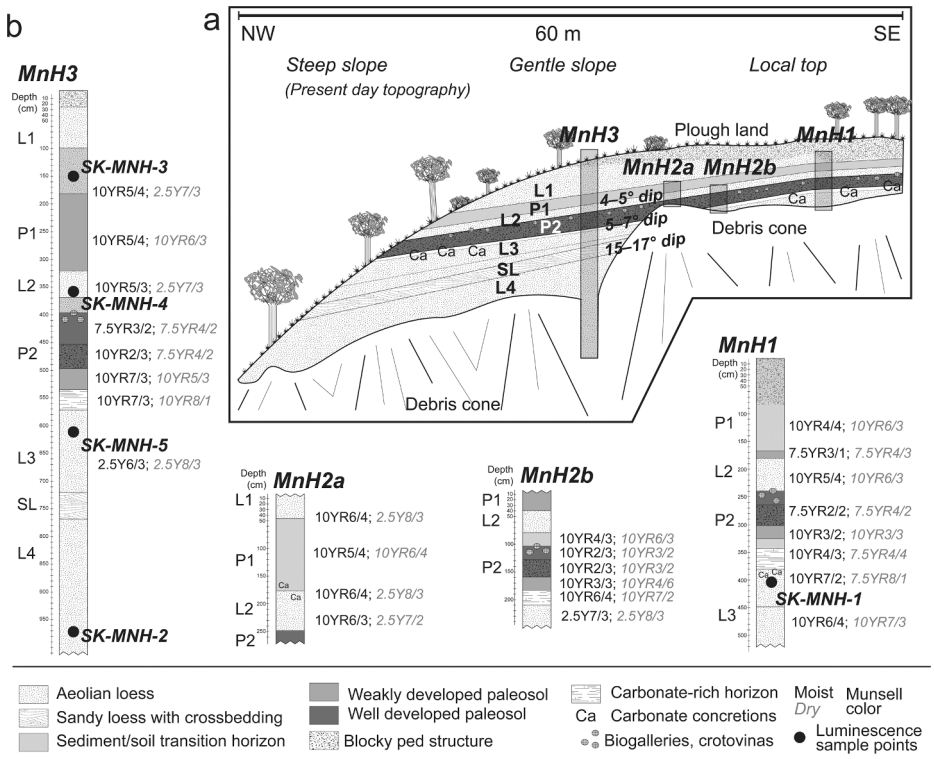


**Fig. 2.** The sketch of the studied loess outcrop in the Malá nad Hronom abandoned brickyard (a) and the graphic log and lithostratigraphical subdivision of the studied profiles (b). Fig. 2a and b have been modified after Szeberényi et al. (2020).

Guérin et al. (2011). An average a-value of 0.08 ± 0.02 (Rees-Jones, 1995) was used for the calculations. The cosmic radiation was corrected for altitude and sediment thickness (Prescott and Hutton, 1994), assuming a water content of 15 ± 5% for all samples (Stevens et al., 2011).

## 4. Results

### 4.1. Characterization of the lithostratigraphical units of the studied succession

Four profiles were cleaned and sampled in the loess outcrop of the Malá nad Hronom brickyard. In terms of observations concerning the recent geomorphology of the neighborhood of the outcrop and the dip of the units under consideration, profile MnH1 is located at the edge of the

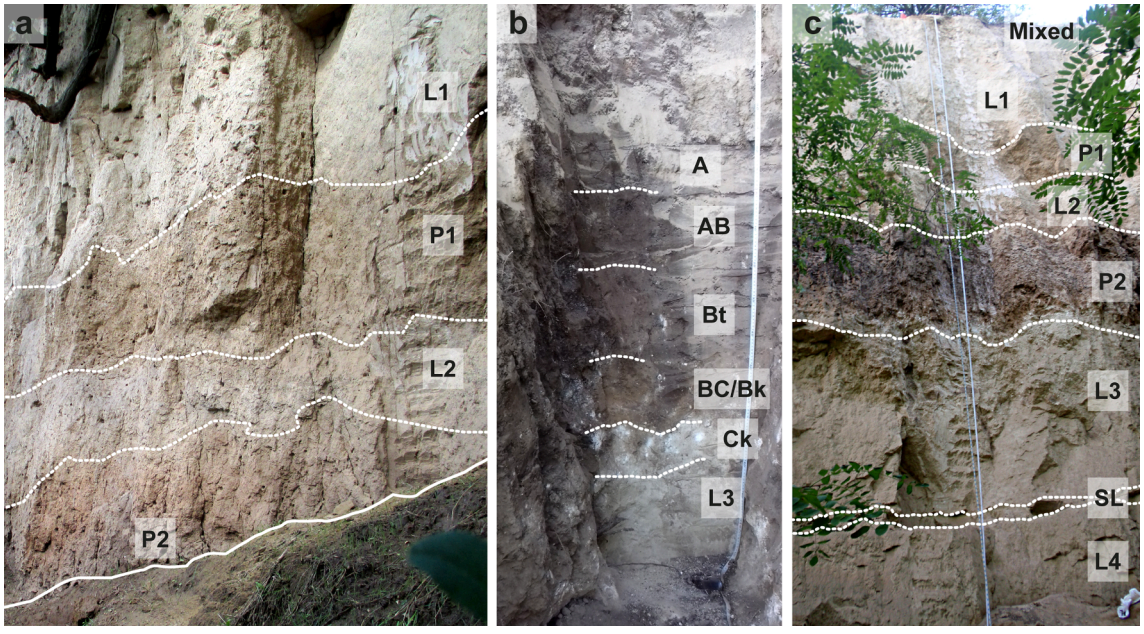


**Fig. 3.** The loess-paleosol section at the Malá nad Hronom outcrop. a) the location of MnH2a and b; b) the excavated P2 Luvisol-like (that is, brown forest soil) paleosol horizon at MnH2a and b profile (A, AB, Bt, BC/Bk, Ck represent the characteristic soil horizons); and c) profile MnH3.

local top. MnH2a and b, which were a part of a quasi-composite section including a well-developed soil (MnH2b) and the overlying sediment unit with a poorly developed soil (MnH2a), are located in a slope position (Fig. 3a, b). As with MnH2a and b, MnH3, the thickest succession of all, is also located in a slope position (Fig. 2a and b; Fig. 3c). There is a decreasing tendency in the dip from the lowermost layers (e.g. SL: 15–17° dip) through the 5–7° dip of the characteristic P2 soil horizon to the lowest 4–5° dip of the poorly developed uppermost P1 paleosol.

The main stratigraphic units of the profiles under consideration can be described as follows (Fig. 2b and 3).

L4 appeared as a thick (>2 m), grey/greyish yellow, loose, homogeneous, sandy loess basal unit in section MnH3 (below ca. 770 cm). L4 was characterized by a secondary carbonate-rich horizon (concretion in 1–2 cm diameter size), biogalleries (maximum 10 cm in diameter, possibly formed during (sub)recent biogene activity) and redox phenomena (manganese patches and dots).

A thin (around 30 cm) SL sandy unit with coarser grains, characterized by a laminated and cross-bedded sedimentary structure, overlay the homogeneous layer L4 (ca. 770–720 cm). An SL unit could only be found in profile MnH3, lying between L4 and the overlaying layer L3.

The characteristics of the L3 loess was very similar to those of L4: a grey/greyish yellow colored, homogeneous fine-grained silt with secondary carbonate cementation. L3 appeared in MnH3 (ca. 570–720 cm) and as a lowermost horizon in MnH2b (below ca. 210 cm) and MnH1 (below ca. 400 cm).

P2 is a well-developed Luvisol-like paleosol layer formed on L3 loess (Fig. 2b and 3b, c). A well-developed ped (aggregate with characteristic shape) structure and different soil horizons were identified in P2. The lowermost horizon of P2 was a well compacted, light yellow/white, well-cemented secondary carbonate-rich horizon (carbonate which is formed during/after the diagenesis of loess and/or by pedogenic processes), identified as Ck (Fig. 3c-Ck). A brown/reddish brown paleosol horizon with weakly developed ped structure overlay the carbonate-rich horizon (Fig. 3c-BC/Bk). The lower boundary of the reddish-brown horizon was abrupt, and the upper boundary was gradual. It was followed by a deep brown colored, clayey pedogenetic horizon (Fig. 3c-Bt). The deep brown horizon had a well-developed blocky soil structure with evidence of 'slip and slide' phenomena on the surface of the peds. The biogallery-rich horizon, overlaying the deep brown subunit, is characterized by biogalleries (around <3 cm diameter) with orange/orange brown clayey silt infill (Fig. 3c-AB). A gradual, irregular upper boundary was observed between the P2 paleosol and the overlying thin L2 loess layer (Fig. 3c-A). The P2 paleosol appeared in all the profiles and could be followed through the entire area of outcrop under consideration (MnH1: ca. 240–380 cm, MnH2a: below ca. 250 cm, MnH2b: ca. 80–210 cm, MnH3: ca. 370–570 cm; Fig. 2b).

L2 was a slightly altered, homogeneous, yellowish silt with secondary carbonate. The boundary between L2 and the weak paleosol P1, developed on L2, was barely detectable macroscopically. L2 appears in all of the studied profiles (MnH1: ca. 185–240 cm, MnH2a: ca. 180–250 cm, MnH2b: ca. 40–80 cm, MnH3: ca. 320–370 cm; Fig. 2b and 3a, c).

The poorly developed Regosol-like paleosol P1 was characterized by a granular ped structure. The uppermost horizon of P1 was a light/middle brown horizon with a grainy ped structure. The boundaries of the horizon were gradual. The thickness of P1 increased from the upper part of the courtyard (about 70–90 cm; MnH1) through MnH2a (ca. 170 cm) to the lower part of the outcrop, where the thickness of horizon P1 reaches about 220 cm (Fig. 2b and 3a, c).

Two different kinds of lithostratigraphic structure were identified in the section overlaying paleosol P1. The recent soil and loess were identified in the uppermost part of profile MnH1. The overlying loose mixture contained different achaeological finds (the possible remains of a fireplace and some fragments of ceramic) and materials of anthropogenic origin. A different sediment sequence was identified in the lower part of the courtyard. In profiles MnH2a and MnH3, the P1 paleosol layer was covered by a well-cemented, homogeneous L1 (uppermost) loess layer. A carbonate concretion horizon was identified in the upper part of layer L1.

Following Schmidt (1968), the whole loess succession of the outcrop may be dated to the Middle/Late Pleistocene transition and the Late Pleistocene and the well-developed P2 paleosol represents the marine isotope stage (MIS)5 (last interglacial) period.

To compare the parameters of the paleosols of MnH profiles, the results were compared with the parameters of the paleosols from the Paks loess profile (Hungary). The Paks loess profile is located in the Middle Danube Basin region of the European Loess Belt and plays an important role in pan-European loess stratigraphy and terrestrial palaeoclimate reconstruction (Marković et al., 2015). In a recent sampling session, started in 2014, a 16-m thick loess/paleosol sequence was investigated, containing paleosols dating back to a period between MIS19 to MIS10 (Újvári et al., 2014). In this study, only the magnetic susceptibility and profile development index of the paleosols were used as a comparison. For a detailed characterization of the so-called Mende Base (MB) paleosol horizon, the Paks sandy soil Complex (Ph1 and Ph2), hydromorphous soil at Paks (Mtp), Paks Double 1 (PD1) and 2 (PD2) paleosols, the parameters of which were used in this study, please see Újvári et al. (2014), Bradák et al. (2018 and 2019) and Supplementary Material 1.

### 4.2. Vertical distribution of the proxies

The vertical change of grain size distribution (GSD) can be described as follows (Fig. 4 and Suppl. Mat. 1):

- GSD indicates well-sorted material, with a dominance of silt. Among the records examined, the average silt component is highest in MnH3 (73%) (MnH1: 67%, MnH2a and b: 67 and 69% respectively).
- The amount of fine sand and coarser grain size components seems insignificant in all the records.
- Along with the highest silt component (see above), the MnH3 succession generally contains significantly less clay (14%) than the others (MnH1: 23%, MhH2a and b: 24 and 23%, respectively).
- Compared to the P2 soil in profile MnH1, no characteristic increase of clay content can be observed in P2 soils from the records MnH2a, b and 3.
- In P1 a slight increase in clay content can be recognized in every section studied.
- Fluctuating clay and silt content can be observed in the P2 and P1 soils in section MnH3.

Compared to the low κlf of sediment units (~0.3–0.4 × $10^{-3}$ SI), a significant increase in κlf can be observed in P2 paleosol horizons in profiles MnH1, 2b and 3 (~1.0–1.2 × $10^{-3}$ SI) (Fig. 5). Compared to the relatively sharp lower transition, the upper transition of MnH2b and MnH3 shows a step-like feature and gradualness. While a clear κlf peak is observable in the P2 paleosol, the P1 horizon is only represented by a slight increase in κlf (~0.5–0.6 × $10^{-3}$ SI), which is difficult to recognize on the upper part of the successions (MnH1, 2a and 3).

The U-ratio shows quite a different pattern to the κlf. Generally, the sediment units are indicated by a higher U-ratio (~1.5) and the paleosols by a lower (~1). This general observation does not, however, apply to the P2 horizon in MnH3, where the paleosol is marked by a fluctuating U-ratio with high peaks (~1–2.5). An irregular case among the P1 soils can be observed in MnH3, where a high peak (~1.5) appears in the middle part of the soil horizon (Fig. 5).

The vertical change in $CaCO_3$ content displays the opposite trend to that of the κlf. Higher values (20–30%) are associated with sediment units, while paleosols, both the P1 and P2 units, have a lower (~10%) $CaCO_3$ content. Sharp peaks of ~30–40% $CaCO_3$ content with a gradual decrease downward can be observed at the lowermost pedogenic horizon of the P2 paleosol units (Fig. 5).

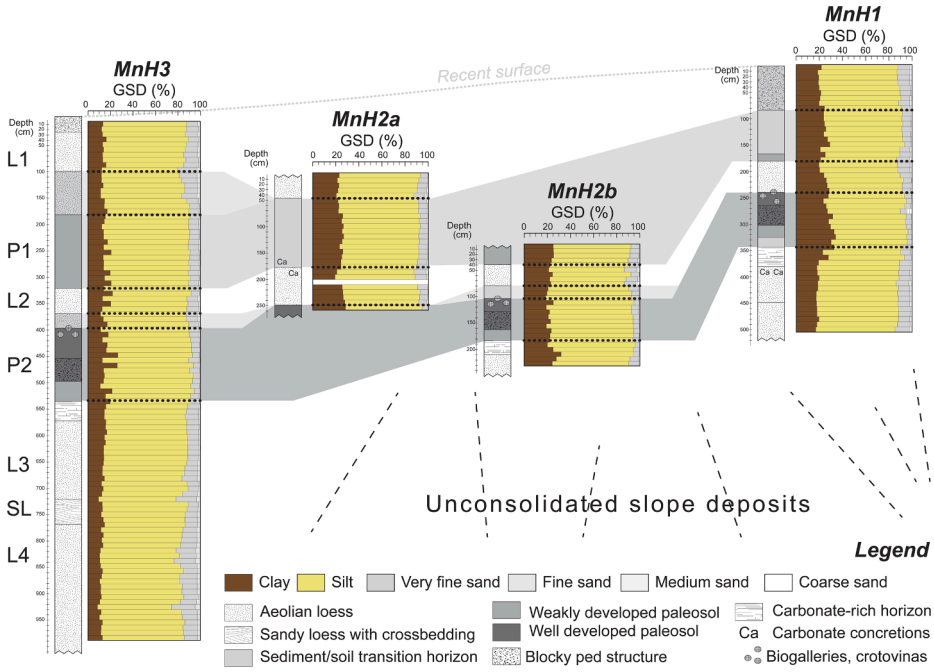


**Fig. 4.** The vertical change in grain size distribution in the sequences examined.

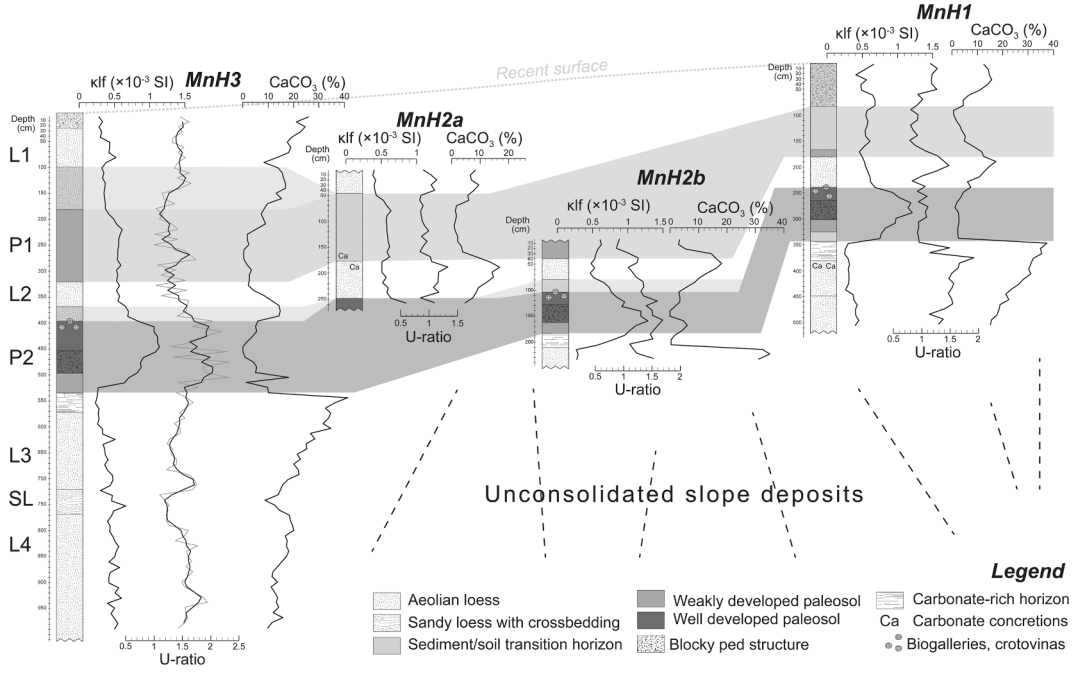


**Fig. 5.** The characteristics of the vertical distribution of pedogenic (κlf), sedimentary (U-ratio) and hydromorphic ($CaCO_3$) environment proxies.

### 4.3. Connection between the proxies

A correlation matrix was used to characterize any connections between the trends and reveal the driving forces behind them observed in the vertical change of the proxies. Pearson's correlation coefficient (r) shows a strong and moderate negative relationship between the pedogenic (κlf) and hydromorphic ($CaCO_3$) proxy in the MnH1 (r = −0.78) and MnH3 (r = −0.64) profiles, consisting of the P1 and the well-developed P2 pedogenic horizons. In MnH2a and MnH2b, which only contain P1 or P2 paleosols, only a weak negative (r = −0.32) relationship was observed, with no statistical significance (r = 0.09) (Suppl. Mat. 3).

A moderate negative relationship was observed between the κlf and U-ratio in MnH1 (r = -0.56), and a moderate positive relationship in profile MnH2b (r = 0.65); a weak positive relationship was noted in MnH3 (r = 0.39) (Suppl. Mat. 3).

A strong positive relationship was observed between the U-ratio and $CaCO_3$ content in the MnH1 (r = 0.76) and 2a (0.74) successions. No statistical relationship could be found between the U-ratio and $CaCO_3$ content in MnH2b (r = −0.17) and 3 (r = −0.05).

Along with the correlation of the κlf, U-ratio and $CaCO_3$ proxies, the relationship between the parameters and various grain size classes was

also investigated (Suppl. Mat. 3).

A strong and moderate positive relationship was found between the κlf and clay content of the units in the MnH1 (r = 0.59) and 2a (r = 0.74), 2b (r = 0.56) profiles, respectively, but in MnH3 the correlation coefficient indicates only a very weak connection (r = 0.27). Along with the increasing κlf (and clay content), decreasing sand content was indicated by the correlation coefficient in MnH1 (κlf vs very fine sand, r = −0.7 and fine sand = −0.57) and MnH2b (κlf vs very fine sand, r = −0.58 and fine sand = −0.45). In MnH2a and 3 only a weak negative relationship was found between κlf and coarser grain components (r = −0.5 to −0.34) (Suppl. Mat. 3).

The U-ratio may be significantly influenced by the change of proportion in clay and sand components in MnH1, as indicated by the correlation coefficient (MnH1: U-ratio vs. clay r = −0.69, U-ratio vs. very fine sand r = 0.64). Such a strong or even a moderate relationship cannot, however, be found between the U-ratio and clay or sand contributors in MnH3 (U-ratio vs. clay r = −0.38, U-ratio vs. very fine sand r = 0.12). In MnH2a and 2b weak and moderate negative statistical relationships were identified between the U-ratio and clay content (r = −0.31 and −0.53), respectively, and a moderate positive relationship between the U-ratio and very fine sand (r = 0.58) in MnH2a, with a negative relationship (r = −0.45) in MnH2b (Suppl. Mat. 3).

### 4.4. Principal component analysis

Through the use of principal component analysis (PCA), the information contained in the dataset was reduced to two variables (Principal Components 1 and 2; Fig. 6). In the case of the data originating from the four studied successions, the "explained variation per principal component", is 45.6% in the first principal component and 22.5% in the second principal component (Suppl. Mat. 4). On the basis of the analysis of "loadings", three parameters, namely, the $CaCO_3$ (PC1), clay and silt (PC2) content of the samples, played the most important roles in the determination of the principal components.

Based on the distribution of the data in Fig. 8, the well-developed P2 paleosol horizons (from all sequences studied) are clearly separated by the sediments and the weakly developed P1 paleosols by their characteristics, as represented by the principal components. Although two recognizable groups, representing the less developed P1 and sediment units, may be discerned the similarities between the two groups are greater, as indicated by the intermixing of the data (Fig. 6). As shown in Table 1, PC1 and 2 were formed on the basis of the three original variables, and do not preserve reliable amounts of information from all of the parameters under consideration, and cannot therefore provide significant material for further interpretation.

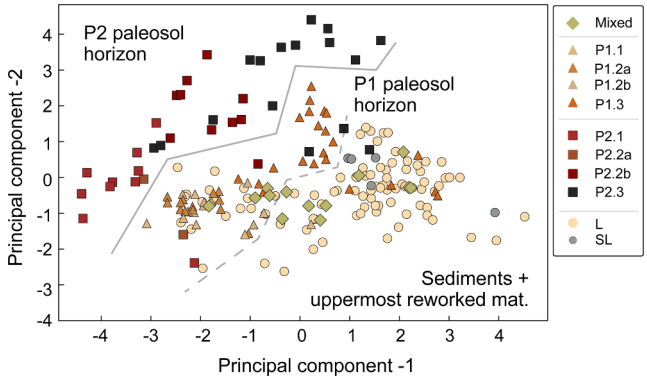


**Fig. 6.** The similarities and differences between the stratigraphic units. Principal components 1 and 2 represent the magnetic susceptibility, carbonate content and grain size parameters, summarized in Supplementary Material 1. P1 and P2 refer to the P1 and P2 paleosol units in MnH1 (0.1), MnH2 (.2a and .2b) and MnH3 (0.3) records, respectively. l indicates the loess units in all profiles; SL indicates the sandy loess horizon in MnH3 and "Mixed" data related to the uppermost reworked unit (further information on the stratigraphic units can be found in Fig. 2).

**Table 1**
The results of luminescence dating. Sample positions can be found at Fig. 2.

| Layer (sequence) | Sample code | Dose rate [Gy/ka] | Equivalent dose [Gy] | pIRIR age (ka) |
|---|---|---|---|---|
| P1, upper (MnH3) | SK-MNH-3 | 4.10 ± 0.19 | 99.1 ± 2.0 | 24.2 ± 1.2 |
| L2 (MnH3) | SK-MNH-4 | 3.79 ± 0.18 | 220.8 ± 4.3 | 58.2 ± 3.0 |
| L3, below P2Ck (MnH1) | SK-MNH-1 | 2.87 ± 0.15 | 406.8 ± 8.0 | 142 ± 8 |
| L3 (MnH3) | SK-MNH-5 | 3.02 ± 0.16 | 478.4 ± 12.6 | 158 ± 9 |
| L4, bottom (MnH3) | SK-MNH-2 | 3.37 ± 0.17 | 569.1 ± 10.6 | 169 ± 9 |

### 4.5. Determination of luminescence ages

The measured U-, Th-, and K-contents and the calculated dose rates are shown in Suppl. Mat. 5. All calculated dose rates, equivalent doses and $pIRIR_{290}$ ages are presented in Table 1. Samples collected from MnH3 (SK-MNH-3,4,5,2) show an age increase with depth. The lowermost two samples are taken from below the P2 soil. A $pIRIR_{290}$ age of 158 ± 9 ka was obtained for sample SK-MNH-5 and 169 ± 9 ka for sample SK-MNH-2, clearly indicating dust deposition during MIS 6. Sample SK-MNH-1 originates from the underlying loess layer of the P2 soil from profile MnH-1. The $pIRIR_{290}$ measurement yielded an age of 142 ± 8 ka for this sample, which ~~also~~ shows that this loess was also deposited during MIS 6 and further confirms that the P2 soils and the underlying loess are identical in both profiles. Sample SK-MNH-4 was taken from the loess between the two paleosol horizons and gave an age of 58.2 ± 3.0 ka. The deposition age of the uppermost transitional horizon is 24.2 ± 1.2 ka (sample SK-MNH-3).

## 5. Discussion

### 5.1. The age of the studied units and their connection to the loess stratigraphy in the ELB (Middle Danube Basin and surroundings)

The youngest loess-paleosol succession, deposited between the Penultimate Glacial (MIS 6) and the end of the Last Glacial (MIS 2), is frequently exposed along the Danube and those tributaries connected to the Danube Bend (e.g. Basaharc, Süttő, Verőce, in the neighborhood of Malá nad Hronom). At Basaharc the uppermost 5–6 m of the succession was deposited between MIS 6 and MIS 2 and contains a thick double-paleosol, the lower part of which was formed during MIS 5 and the upper part during MIS 3 (Frechen et al., 1997, Novothny et al., in preparation). In the same time interval much thicker and detailed sequences were deposited and formed at Süttő (~20 m) and Verőce (~12 m) (Novothny et al., 2009, 2011; Bradák et al., 2014; Barta et al., 2018), where the MIS 5 and 3 paleosols also appear separately and the MIS 5 pedocomplex contains the paleosol which formed during MIS 5e. This latter, reddish brown paleosol is usually missing from the loess sequences exposed in the Middle Danube Basin and is preserved only at these two profiles, as far as is known.

Judging by its thickness (5–10 m) and appearance of the included paleosols, the loess profile at Malá nad Hronom, represents a transition between the well-developed and preserved profiles at Süttő and Verőce and the less well preserved profile at Basaharc. In contrast to the Basaharc profile, the dust deposited during MIS 4 is retained here in a thickness of 0.5 m. This might indicate either more significant dust deposition during that time or less intensive erosion subsequently, compared to Basaharc. However, the thickness of the MIS 4 loess here is still minor compared to Süttő. Granulometry results (higher sand

content of this sediment) also indicate higher wind speeds (or coarser source material) at Süttő compared to Malá nad Hronom during MIS 4.

On the basis of the $pIRIR_{290}$ ages the P1 paleosol was formed during MIS 3. The thickness and development of this paleosol are similar to those profiles where the MIS 3 paleosol is preserved as an independent layer, such as at Albertirsa, Bodrogkeresztúr, Dunaszekcső and Süttő in Hungary (Bösken et al., 2019; Novothny et al., 2009, 2011, 2002; Újvári et al., 2014), various profiles in Austria (Terhorst et al., 2015 and the references therein), at Nussloch in Germany (Antoine et al., 2009a), in the Zeměchy and Dobšice sections in the Czech Republic (Hošek et al., 2015), at in numerous sections in Poland and Ukraine (e.g. Jary and Ciszek, 2013) and in Serbia (Antoine et al., 2009b; Marković et al., 2015 and the references therein). In the neighborhood of Malá nad Hronom, a very detailed MIS3 is represented in the Bíňa loess section, where a unique soil complex was preserved in a paleochannel and a soil horizon was formed in a paleoslope position (Hošek et al., 2017). Although the thickness and development of such paleosol horizons make the units a significant stratigraphic marker horizon, there are differences in their pedogenic character due to the differences in the pedogenic environment (e.g. paleoclimatic differences) between the regions studied. MIS 3 is represented by a weakly developed Bw horizon of Cambisol in Serbian loess (e.g. Antoine et al., 2009a), but appears as variations of a subartic brown, gleyey soil in the loess sections in Poland (Jary and Ciszek, 2013). In the Middle Danube Basin and the Central European region of the European Loess Belt, Cambisol seems to be one of the most common soil types, representing MIS 3 (e.g. Bradák et al., 2014; Hošek et al., 2015 and some study cited above). As suggested by Terhorst et al. (2015), the characterization and comparison of MIS 3 paleosol horizons may play a key role in future regional level environment reconstructions.

The $pIRIR_{290}$ age (24.2 ± 1.2 ka) of the transitional horizon above the P1 paleosol at MnH3 indicates that soil formation was competing with sedimentation during the early part of MIS 2, at least for the lower slope position, which resulted in the extraordinary total thickness of this soil.

### 5.2. Relationship between sedimentation and pedogenesis

Given the moderate to strong relationship between κlf and $CaCO_3$, and the fact that in most of the studied successions $CaCO_3$ content is lower in paleosol units, this suggests the operation of vertical hydromorphic processes during and/or after pedogenesis. The presence of such vertical processes is supported by the characteristic $CaCO_3$-rich horizons observed below the P2 units and defined as Ck (or Bk) pedogenic horizons. Ck pedogenic horizon can be observed in "forest soils" (Luvisols; IUSS Working Group WRB, 2015), indicating high precipitation and humid climate during the development of the paleosol. These factors may then, in turn, cause an increase in the intensity of weathering, as indicated by the increasing clay content in the well-developed P2 paleosol in profiles MnH1 and MnH2b but not in MnH3. The moderate or strong relationship between κlf and clay content parameters in MnH1, 2a and b tends to confirm the correctness of the use of the pedogenic enhancement model in relation to the magnetic susceptibility signal of the paleosols, i.e. the neoforming and enrichment of magnetic contributors by pedogenic processes (weathering and bacterial activity) during humid and warm (moderate) periods of the Pleistocene (e.g. Evans, 2001 and the references therein). The P2 paleosol, formed during MIS 5e, represents an interglacial period characterized by humid and moderate/warm climate in the region. Along with the increasing clay content, a decrease in coarser grain (sand) components was notified in MnH1 and 2b. This suggests the weathering of coarser grained components and/or the decreasing of the activity of surface processes which carry coarser grains during periods of soil formation.

The connection between the U-ratio (i.e. the increasing or decreasing intensity of dust sedimentation; Vandenberghe et al., 1997) and the change in clay/very fine sand components may indicate the influence of changing pedogenic/sedimentary environments during the development of the succession. In MnH1 and 2b the change in the U-ratio is significantly influenced by the strengthening of pedogenic processes during warmer, humid periods, as indicated by e.g. the increasing κlf and clay component parameters (Fig. 5 and Suppl. Mat. 3a, c). The moderate/strong positive relationship between the U-ratio and e.g. very fine sand in MnH1 and 2a may be interpreted as the mark of the influence of increasing sediment input and intensification of sedimentary processes during colder and drier glacial periods. Such influences are not so clearly visible in MnH3. The weak and modearate statistical relationship between the U-ratio and clay/(very) fine sand components and the irregular trends, increasing κlf and U-ratio in the P2 unit of MnH3, suggest that pedogenic and sedimentary processes may have appeared in parallel during the development of MnH3 succession (Fig. 5 and Suppl. Mat. 3d).

The behavior of various proxies (with the focus on κlf and the U-ratio) in MnH1 follows the trend as reported for various loess successions from within the vicinity of the profile in the ELB. A κlf peak associated with a low U-ratio has been described in the well-developed MIS 5 paleosol (complex) at Süttő (Hungary) (Novothny et al., 2011), in the lowermost MIS 3 paleosol at Bodrogkeresztúr (Hungary) (Bösken et al., 2019), and also in the lowermost paleosol of the Sand Pit loess series in Susak (Croatia) (Wacha et al., 2018). As with the Late Pleistocene examples previously mentioned, the "Basal soil complex2" (MIS 5) and "Middle Soil complex" (formed in MIS 3 and/or 2) in the Surduk loess profile (Serbia) are characterized by increasing susceptibility associated with fine grain components (Antoine et al., 2009b). The same phenomenon has been observed in the well-developed MIS 5 paleosol in the Mošorin and Titel loess profiles (Serbia) (Bokhorst et al., 2011).

The relationship between κlf and the U-ratio in these loess profiles clearly reflects the relationship between sedimentation and pedogenesis in glacial and interglacial periods. Glacial periods are characterized by increasing coarser grain (sandy loess, fine sand) input and a growing sedimentation rate without significant pedogenesis and the formation of (relatively) well-developed paleosols. In contrast, it is believed that paleosols are formed during periods characterized by reduced sedimentation in a more humid climate. Such a theory applies especially to, for example, so-called plateau loess, "where loess deposition was a relatively stable process and preservation potential highest" (Marković et al., 2015, p. 231) and the development of the sequence is not influenced by significant erosion or an unusual rate of sediment accumulation due to slope processes or geomorphological position (e.g. Terhorst et al., 2014). On the basis of the parameters examined here (Figs. 4 and 5), the MnH1 section represents first and foremost a plateau loess-like succession characterized by well separable pedogenic and sedimentary periods around the first part of the Late Pleistocene.

In the case of the P2 paleosol in MnH3 and also in profile 2b, the parallel increase in κlf and the U-ratio (Fig. 5) suggests the appearance of pedogenic processes and increasing sediment input at the same time, accompanied with strong lessivage (leaching), as indicated by the change in $CaCO_3$ content and the Ck (Bk) accumulation horizon. A similar feature can be observed e.g. in the upper part of Bodrogkeresztúr foothill loess succession, where a parallel increase in κlf and the U-ratio is discernable in the poorly developed paleosol/weathered horizon (Bösken et al., 2019).

### 5.3. Influence of various environmental factors on pedogenesis

The development of the P2 and P1 paleosols during continuous sediment input can be described by a model of soil formation in an aggradational sedimentary environment. The formation of paleosols can be described as the balance between the sediment accumulation and the rate of pedogenesis (from various geological periods and facies: Morrison, 1978; Bown and Kraus, 1981; Marriott and Wright, 1993; Wright and Marriott, 1996; Kraus, 1999). In cases of insignificant erosion and rapid, unsteady sedimentation, so-called compound paleosols can form (sed. > ped.). When the rate of pedogenesis and sedimentation are close

to each other, composite paleosols may form (ped.≈ sed., unsteady sedimentation). In addition, if there is no or only insignificant erosion and the sedimentation rate is steady, cumulic soils can develop (ped. ≥ sed, steady sedimentation).

In MnH3 and 2a and b, pedogenic processes might have kept working in parallel to increasing sedimentation during the transition period between interglacial and glacial phases (P2) and during a moderate, humid period which interrupts the dry, cold glacial phase (P1). Together with increasing aeolian sedimentation, pedogenesis may form compound/cumulative paleosol horizons. As shown by the relation between the pedogenic (κlf) and the sedimentation proxy (U-ratio) in P2 from MnH3 and 2b, the cumulative character of a paleosol might not only be limited to the transition period, but may extend over the entire phase of pedogenesis due to the quasi-permanent sediment input during the last interglacial. The discussion of dust accumulation during pedogenic (interglacial/interstadial) periods is not common in literature concerning loess successions, but there are some studies which describe its potential influence in pedogenesis (see below).

In the case of "The Palouse loess region" (United States), which is the downwind region of the Channeled Scabland, and is strongly influenced by repeated floods from Glacial Lake Missoula, both climate cycles and catastrophic events affected the characteristics of sedimentation and pedogenesis during warmer periods of Quaternary (Busacca, 1989). Changes in the characteristics of pedogenesis have been reported in Holocene soils in Alaska (Matanuska Valley), influenced by the increasing dust influx in locations closer to the sediment source (silts are produced through grinding by the Matanuska and Knik glaciers) (Muhs et al., 2004, 2016). The unmixed nature of grain size distribution curves from a loess succession on the Tibetan Plateau revealed the deposition of fine-grained loess component (medium silty loess) during interglacial periods and has been defined as background sedimentation (Vriend and Prins, 2005). The observation concerning the constant flux of fine-grained components (background sedimentation) during interglacials has also been expanded to the region of the Chinese Loess Plateau (especially its central and southern parts) (Prins et al., 2007). Almond and Tonkin (1999) and Eger et al. (2012) report accumulative (upbuilding) pedogenesis as a response to an active loess flux in a humid environment in New Zealand loess.

In the European Loess Belt, the mark of interglacial dust accumulation was identified in Middle Pleistocene soils from the Paks loess profile (Hungary) by Varga et al. (2016). Increasing sedimentation was identified in the Dunaszekcső profile during MIS5 soil formation, as well (Újvári et al., 2019). A study by Zech et al. (2013) challenges the "traditional" view of the warm, humid interglacial and cold, arid interglacial periods by introducing the notion of an arid pedogenic environment during MIS 3 and MIS 5 on the evidence of the Crvenka loess (Serbia). The Malá nad Hronom loess succession may well be connected to this. Differences in sedimentary environment, followed by differences in paleosol formation and pedogenic characteristics may be interpreted as differences in paleoclimate. Revealing the relationship (balance) between sedimentation and pedogenesis may help to characterize the influence of local topography during soil formation under uniform paleoclimatic conditions.

As proposed by Verosub et al. (1993) and supported by the examples above, loess sedimentation and paleosol formation are essentially competing processes: during glacials, dust deposition is dominant, during interglacials, pedogenesis is stronger, but both processes proceed simultaneously.

There is one question remaining, namely, how much the advent of increasing sedimentation changes the pedogenic character of the forming paleosol. Comparing various proxies of pedogenesis, i.e. the Harden index and κlf, no significant differences can be found between the same paleosol horizons originating in sequences located in the top, slope or local depression topographic positions.

The connection between the horizon indices, calculated for every pedogenic horizon of the paleosol being examined, and their susceptibility values displays similar trends in all the sequences examined in this study (Fig. 7). This observation suggests that increasing sediment input may also increase the thickness of the profile (e.g. in the Polanów Samborzecki sections, Jary and Ciszek, 2013; in Verőce, Bradák et al., 2014). In the Malá nad Hronom loess profile the increasing sediment income did not significantly change the character of pedogenesis and pedogenic sub horizons; neither did it affect the trend of the κlf curve in the cumulative paleosols. In Fig. 7, a slight decrease in the development of the subhorizons in MnH3 can be observed (associated with the same maximum κlf in all studied P2), possibly triggered by continuous sediment income during pedogenesis, which would operate to weaken the soil development index. This sediment income might not significantly influence weathering and pedogenic mineral neoforming processes indicated by κlf, which displays the same peak value as the P2 soil in MnH1 and 2b (Figs. 5 and 7). Compared, for example, to the Polanów Samborzecki section (Poland), where the marks of cryoturbation and solifluction can be observed (Jary and Ciszek, 2013), and Verőce (Hungary), where water-lain processes are responsible for the increasing sediment input (Bradák et al., 2014), no such marks can be observed at Malá nad Hronom. The lack of mass movements, cryogenic and water-lain processes suggests that aeolian transportation might be responsible for the increasing sediment input.

Comparing the relationship between the κlf and Harden parameters (HI and PDI) from soil horizons in the case of the Paks succession (Hungary) and the Malá nad Hronom loess, similar tendencies can be observed between MnH1, 2 and the Paks paleosols. Such similarity may suggest a relationship between sedimentation and pedogenesis in the pedogenic environment during the development of e.g. the P2 paleosols and the Mtp and PD1 horizons at Paks (Fig. 7).

### 5.4. *The simplified model of the dynamic microenvironment at Malá nad Hronom*

The GSD and its vertical change in the successions under consideration reveal the following basic information about the sedimentary and pedogenic environment:

- The well-sorted character of the sediments (and paleosols), along with the dominance of the silt component, suggests aeolian sedimentation (e.g. dust falls), which appear to be most intense in the MnH3 section (indicated by the significantly higher silt content compared to other records).
- The lack of a coarser sand grain component (average of fine sand and coarser fractions: 1–2%) also supports the supposition of an aeolian origin for the sediment and may exclude the redeposition of the material by water-lain processes (e.g. Vandenberghe, 2013).
- In Malá nad Hronom, MIS 6 and 2 are represented by similar sand components. This result differs from some profiles from the vicinity of Malá nad Hronom, such as the Süttő section (Novothny et al, 2011), where MIS 6 and 4 show similar sand distributions, which then decreases in MIS 2, or the Basaharc section, where a part of MIS 6 loess is characterized by significantly higher sand content (Novothny et al., in preparation).
- The GSD of SL unit does not display significant differences than the loess layers but does exhibit a laminated (with partly cross-bedding) sedimentary structure. This suggests the appearance of a transport medium with a higher transport energy than dust deposition and/or might differ from aeolian deposition, and was able to redeposit the dust on the slope. The formation of SL is possibly related to water-lain processes, which indicates a slightly humid period (or an event) during MIS6.
- The significantly lower average value for the clay component of MnH3 (14% compared to 23–24% in MnH1,2a and b – along with the highest silt component, see above) suggests a lower degree of weathering in MnH3, possibly due to the appearance of quasi-continuous sediment input during pedogenesis.

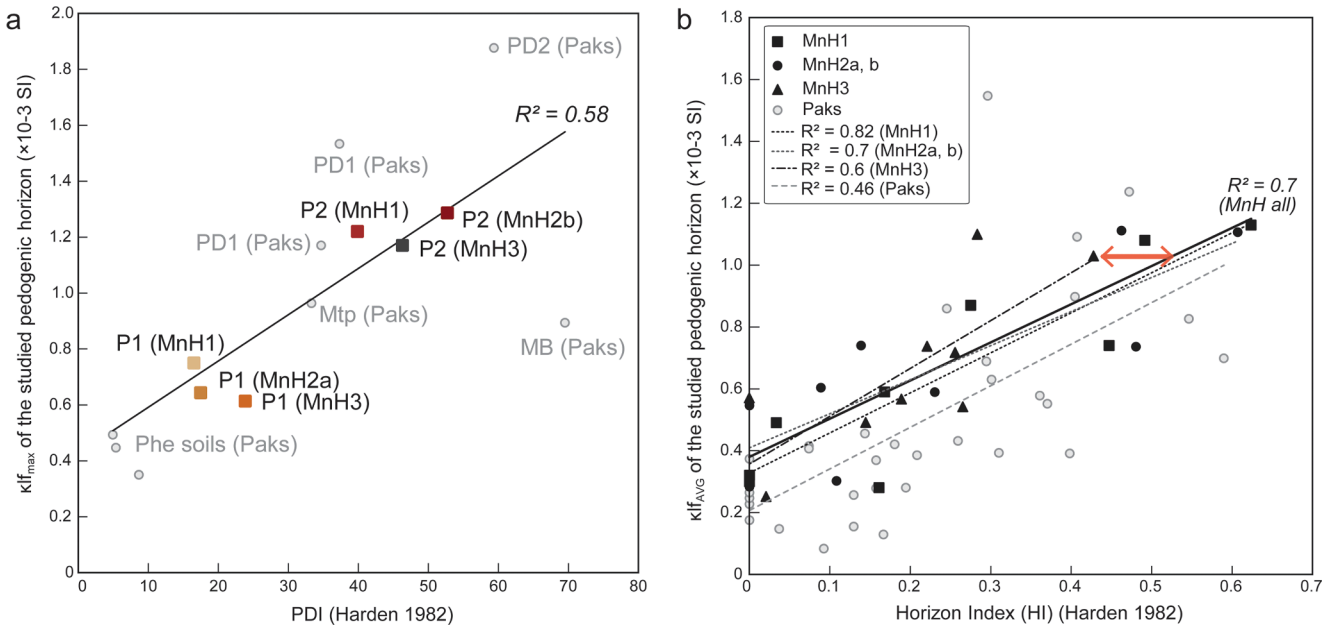


**Fig. 7.** Relation of pedogenic indices of the P1 and P2 paleosols in the Malá nad Hronom loess profile. a) The low field magnetic susceptibility and the Harden index (PDI) of paleosols P1 and P2; b) the connection between the alteration of various pedogenic sub-horizons and their low field magnetic susceptibility value in the MnH1, 2a,b, and 3 sequences. The red double-headed arrow in Fig. 7b indicates the discrepancy between the pedogenic enhancement trend of MnH3 and the other sections, MnH1 and MnH2a,b. (For interpretation of the references to color in this figure legend, the reader is referred to the web version of this article.)

- Such quasi-continuous sediment input (perhaps in a slope topographic position) might cause the lack of clay "peaks" in P2 in MnH2a, b and MnH3, compared to the MnH1 profile.
- The appearance of a P1 weathered horizon can be recognized by the slight increase of clay in every examined section, indicating a short, moderate, slightly humid period.
- The fluctuating clay and silt content observed in the P2 and P1 soils in the MnH3 succession may indicate the rhythm of increasing and decreasing sediment input along with the weakening and strengthening of pedogenesis.

On the basis of the relationship between the parameters examined in this study (Fig. 5 and Suppl. Mat. 3), the following different sedimentary/pedogenic environments can be identified from the Late Pleistocene in the Malá nad Hronom loess outcrop (Table 2, Fig. 8). Due to their proximity to each other (they are in the same outcrop), all of the sequences are likely to have been influenced by the same main climatic characteristics and suffered the effects of climate components, such as precipitation triggered sheet-wash processes and wind erosion, to the same degree. The differences in the degree of such processes is therefore likely to have been determined mainly by the paleogeomorphological positions of the profiles.

The MnH1 sequence represents a "plateau loess" type (here, local top) microenvironment with increasing sedimentation during cold, dry (glacial) periods and pedogenesis during the more humid, moderate/warm (interglacial) phases. The lack of a thick upper transitional horizon in P2 suggests increasing surface erosion or the lack of dust accumulation in the early period of the subsequent colder phase (MIS 5[e] to a more recent colder phase). Sheet-wash processes might have been responsible for the increasing erosion during the transition, but the lack of laminated units (consisting of sediment and paleosol laminas) as characteristic marks of water-lain processes (e.g. Bradák et al., 2011) in lower paleotopographic positions, e.g. in the MnH3 succession, might support the latter theory. Instead of laminated material, the upper transition horizon of P2 in MnH3 and 2b is relatively thick (ca. 30 cm) and characterized by a gradually changing pedogenic to sedimentary character. The dominance of silt and fine sand components, which suggests thorough sorting, may indicate the increasing dust input by

**Table 2**
Paleoenvironmental characteristics in the microenvironment of the Malá nad Hronom succession based on the proxies and parameters examined herein.

| Age (unit) | Key characteristics | Environmental information |
|---|---|---|
| Holocene/ Anthropocene | Surface erosion, mixing of uppermost layers; human activity | Intense erosion in higher topographic positions (e.g. missing L1 in MnH1); Increasing influence of human activity (Anthropocene) |
| MIS 2 (L1) | Dust accumulation and wind erosion (MIS2) | Dust accumulation in lower topographic positions (e.g. in MnH3); in higher topographic position erosion/wind deflation |
| MIS 3 (P1 – Regosol-like paleosol) | Weak pedogenesis and quasi-constant dust accumulation | Moderate temperature, slightly humid period with weak weathering |
| MIS 4 (L2) | Short period, characterized by dust accumulation (+erosion or/and wind deflation, indicated by the thickness of the layer) | Cold, dry period, possibly interrupted by heavy rainfalls (water-lain erosion) or harsh windstorm (wind erosion) event(s) |
| MIS 5/MIS 4 trans. (P2/L2 trans.) | Increasing aeolian sedimentation (e.g. in MnH3, P2 upper horizon) and surface erosion (e.g. MnH1, P2) determined by topographical differences | Aridification toward MIS4, along with surface erosion, possibly triggered by heavy rainfalls and the change of vegetation (e.g. decreasing density of forests) |
| MIS 5 (P2 – Luvisol-like paleosol) | Intense pedogenesis (in all sequences), but constant sediment input on slopes or in local depressions ("sediment trap") (e.g. in MnH3) | Increasing precipitation and weathering; warm, humid environment; but the effects of aeolian activity, driven by topographical differences, cannot be excluded |
| MIS 6 (L4, SL and L3) | Aeolian sedimentation; possible erosional/wind erosion event indicated by the cross laminated sandy layer (in MnH3) | Low precipitation; weak weathering; abrupt climate event (cooling with intense wind erosion) |

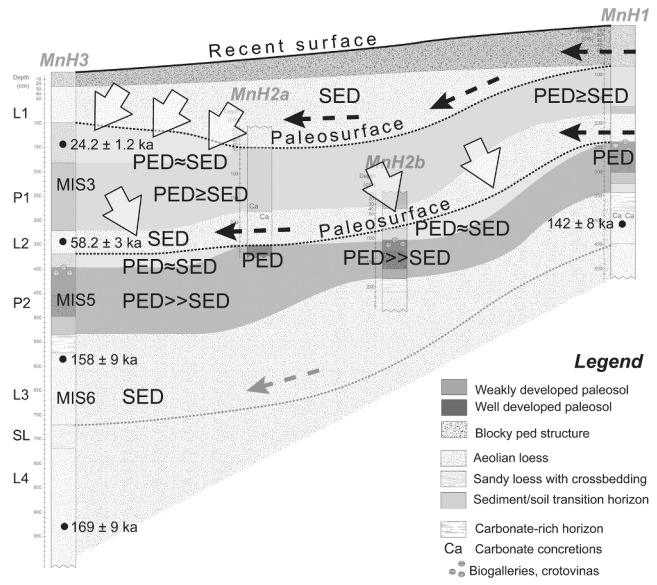


**Fig. 8.** The development of the dynamic aggradational microenvironment in the Malá nad Hronom profile. This is a theoretical model of the relation of sedimentary and pedogenic environments in various topographic positions. The thick white arrows indicate sediment accumulation (dust); the arrows with dashed lines indicate erosion (wind erosion and/or water-lain processes); SED - dominant sedimentation (with very weak weathering); PED ≈ SED - composite soil formation; PED ≥ SED - cumulative soil formation; PED ≫ SED - dominant pedogenesis; PED - pedogenesis (associated with possible surface erosion), Paleosurface - indicates the character of the theoretical surface based on the character of the paleosols in various parts of the outcrop. The reconstructed paleotopography is indicated by the dotted paleosurface lines.

aeolian processes in the MnH3 sequence, e.g. during the drier (stadial, e. g. MIS5d and b) periods of MIS5. The influence of sheet-wash processes which might redeposit the already accumulated, well-sorted loess, cannot be excluded during the humid periods of the MIS 5, either. The increasing aeolian sedimentation and/or the redeposition of loess affected those sequences which are located in a lower paleotopographical position compared to MnH1 (Fig. 4 and Suppl. Mat. 6a). As shown in Suppl. Mat. 6a, the P2 horizon from MnH1 is indicated by increased clay content compared to its parent material. Although a "clay step" can be identified in P2 from MnH3 as well, it contains a significant amount of silt and fine sand compared to its parent material (and P2 in MnH1). Such a significant level of silt and fine sand content, the well-sorted character of grain size distribution curve (indicating an aeolian origin), the peak of κlf and the PDI of P2 from MnH3, (similar to P2 in MhH1, indicating strong pedogenesis; Fig. 7) support the theory: sediment input runs in parallel to intense pedogenesis during the formation of P2 in MnH3 in MIS 5. This increasing sediment input is not limited to the period of the P2 to L2 transition but appears in the period of P1 formation. P1, observed in the MnH3 sequence is significantly thicker and characterized by lower clay and slightly higher very fine sand content compared to P1 horizons in MnH1 and 2a,b (Suppl. Mat. 6b).

The conclusions above emphasize the role of paleotopography in sedimentation and pedogenesis, i.e. the sequences in slope (MnH2a, d) or lower slope (MnH3) topographic position, which act as sediment traps even during moderate, more humid phases. In the case of the succession studied here, the alluvial plain of the Hron might have been a local source of fine grained dust. In cold phases, decreasing vegetation cover and the changing river characteristics (e.g. meandering into a braided channel river) may have provided additional source areas of dust. The theory about a close dust source seems to be supported by the characteristics of the grain size distribution curves in Suppl. Mat. 7. In accordance with the classification of Vandenberghe (2013), L3 (the parent material of P2) falls into the category of "Loess sediments in the medium-to coarse-grained silt fraction (sediment type 1.b)" (Vandenberghe, 2013, p. 23; Smalley et al., 2009).

## 6. Conclusion

Due to its geomorphological characteristics, the Malá nad Hronom loess succession (Slovakia) provided a good opportunity to investigate differences in soil development in various topographic positions. Two paleosols, one well developed, the other less so, were identified in the profile, which was formed in MIS 5 and 3.

Of the mathematical/statistical methods used on the data, the correlation matrix/heatmap provided significant information about the formation of the section, but the use of PCA was not feasible. The key paleoenvironmental information provided by the analyses of the various proxies and the soil development indices can be summarized as follows:

- In the case of the paleosol, which is located in a lower slope position, quasi permanent sediment input was identified, even during soil formation. Such sediment input seems to be surpassed by pedogenesis, a process strengthened by the climate of MIS 5. Pedogenesis seems to keep up with intense dust accumulation once again during MIS 3, but compared to MIS 5, the climate does not favor intense pedogenesis.
- In general, the conclusions arrived at in this study concerning the dynamic aggradational microenvironment of Malá nad Hronom succession support the pioneering theory of Verosub et al. (1993) about the simultaneous and competing appearance of dust deposition and pedogenesis during glacial and interglacial periods.
- Despite the general belief that loess series formed in a plateau position will preserve terrestrial records without significant erosion, in the case of Malá nad Hronom (and also e.g. Süttő and Verőce), it happened differently: a comparison of the sequence affected by erosional events in local top position with the sequence affected by quasi-continuous sediment input in lower slope position shows that the latter appears to have been where the soil horizons were preserved intact.
- The paleosols developed in local top or slope topographical positions did not display significant differences in their degree of development and magnetic susceptibility parameters, that is, in the case of the proxies which can be used to characterize interglacial periods.

Although loess successions formed in (paleo)slope positions are not in the spotlight of studies with a focus on climate reconstruction, a study of the paleosols of the Malá nad Hronom loess section suggests that they can indeed preserve information about the development of paleoenvironment, information concerning changes in sedimentary processes or local topography. The results from Malá nad Hronom also prove that in some cases, surface processes might not significantly change the character of paleosols; they do, however, show that, in common with plateau loess, "slope-sections" can be used in stratigraphic analysis.

## Declaration of Competing Interest

The authors declare that they have no known competing financial interests or personal relationships that could have appeared to influence the work reported in this paper.

*Acknowledgements*

This research was carried out within the framework of the International Visegrad Fund (project Number 11410020). The paper was also supported by a long-term conceptual development subvention available to research organizations RVO: 68145535 from the Institute of Geonics AS CR, by the Slovak Research and Development Agency under contract No. APVV-0625-11 (project "A new synthesis of the Western Carpathians landform evolution – preparation of the database for testing of

key hypotheses".

B. Bradák acknowledges the financial support of project BU235P18 (Junta de Castilla y Leon, Spain) and the European Regional Development Fund (ERD), project PID2019-108753GB-C21 / AECI / 10.13039/501100011033 of the Agencia Estatal de Investigación and project PID2019-105796GB-100 / AECI / 10.13039/501100011033 of the Agencia Estatal de Investigación.

The gamma-spectrometry measurements were carried out at the Leibniz Institute for Applied Geophysics, Hannover, Germany.

We are also thankful for the inspiring ideas and comments of our anonymous reviewers.

## Appendix A. Supplementary data

Supplementary data to this article can be found online at https://doi.org/10.1016/j.catena.2020.105087.

## References

Almond, P.C., Tonkin, P.J., 1999. Pedogenesis by upbuilding in an extreme leaching and weathering environment, and slow loess accretion, south Westland. New Zealand. https://doi.org/10.1016/S0016-7061(99)00016-6.

Antoine, P., Rousseau, D.-D., Moine, O., Kunesch, S., Hatté, C., Lang, A., Tissoux, H., Zöller, L., 2009a. Rapid and cyclic aeolian deposition during the Last Glacial in European loess: a high-resolution record from Nussloch, Germany. Quat. Sci. Rev. 28, 2955–2973.

Antoine, P., Rousseau, D.-D., Fuchs, M., Hatté, C., Gauthier, C., Marković, S.B., Jovanović, M., Gaudenyi, T., Moine, O., Rossignol, J., 2009b. High-resolution record of the last climatic cycle in the southern Carpathian Basin (Surduk, Vojvodina, Serbia). Quat. Int. 198, 19–36. https://doi.org/10.1016/j.quaint.2008.12.008.

Balsam, W.L., Ellwood, B.B., Ji, J., Williams, E.R., Long, X., El Hassani, A., 2011. Magnetic susceptibility as a proxy for rainfall: Worldwide data from tropical and temperate climate. Quat. Sci. Rev. 30, 2732–2744. https://doi.org/10.1016/j.quascirev.2011.06.002.

Barta, G., Bradák, B., Novothny, Á., Markó, A., Szeberényi, J., Kiss, K., Kovács, J., 2018. The influence of paleogeomorphology on the stable isotope signals of paleosols. Geoderma 330, 221–231.

Bokhorst, M.P., Vandenberghe, J., Sümegi, P., Łanczont, M., Gerasimenko, M.P., Matviishina, Z.N., Marković, S.B., Frechen, M., 2011. Atmospheric circulation patterns in central and eastern Europe during the Weichselian Pleniglacial inferred from loess grain-size records. Quat. Int. 234, 62–74. https://doi.org/10.1016/j.quaint.2010.07.018.

Bösken, J., Obreht, I., Zeeden, C., Klasen, N., Hambach, U., Sümegi, P., Lehmkuhl, F., 2019. High-resolution paleoclimatic proxy data from the MIS3/2 transition recorded in northeastern Hungarian loess. Quat. Int. 502, 95–107. https://doi.org/10.1016/j.quaint.2017.12.008.

Bradák, B., Thamó-Bozsó, E., Kovács, J., Márton, E., Csillag, G., Horváth, E., 2011. Characteristics of Pleistocene climate cycles identified in Cérna Valley loess-paleosol section (Vértesacsa, Hungary). Quat. Int. 234, 86–97.

Bradák, B., Kiss, K., Barta, G., Varga, G.y., Szeberényi, J., Józsa, S., Novothny, Á., Kovács, J., Markó, A., Mészáros, E., Szalai, Z., 2014. Different paleoenvironments of Late Pleistocene age identified in Verőce outcrop, Hungary – Preliminary results. Quat. Int. 319, 119–136.

Bradák, B., Seto, Y., Hyodo, M., Szeberényi, J., 2018. Significance of ultrafine grains in the magnetic fabric of paleosols. Geoderma 330, 125–213.

Bradák, B., Seto, Y., Nawrocki, J., 2019. Significant pedogenic and palaeoenvironmental changes during the early Middle Pleistocene in Central Europe. Palaeogeogr. Palaeoclimatol. Palaeoecol. 534, 109335. https://doi.org/10.1016/j.palaeo.2019.109335.

Bradák-Hayashi, B., Biró, T., Horváth, E., Végh, T., Csillag, G., 2016. New aspects of the interpretation of the loess magnetic fabric, Cérna Valley succession, Hungary. Quat. Res. 86, 348–358.

Bown, T.M., Kraus, M.J., 1981. Lower Eocene alluvial paleosols Willwood Formation, northwest Wyoming, USA. and their significance for paleoecology paleoclimatology, and basin analysis. Palaeogeogr., Palaeoclimatol. Palaeoecol. 34, 1–30.

Busacca, A.J., 1989. Long quaternary record in Eastern Washington, U.S.A., interpreted from multiple buried paleosols in loess. Geoderma 45, 105–122.

Buylaert, J.P., Murray, A.S., Thomsen, K.J., Jain, M., 2009. Testing the potential of an elevated temperature IRSL signal from K-feldspar. Radiat. Meas. 44, 560–565.

Buylaert, J.-P., Jain, M., Murray, A.S., Thomsen, K.J., Thiel, C., Sohbati, R., 2012. A robust feldspar luminescence dating method for Middle and Late Pleistocene sediments. Boreas 41, 435–451.

Csonka, D., Bradák, B., Barta, G., Szeberényi, J., Novothny, Á., Végh, T., Süle, G.T., Horváth, E., 2020. A multi-proxy study on polygenetic middle-to late pleistocene paleosols in the Hévízgyörk loess-paleosol sequence (Hungary). Quat. Int. 552, 25–35. https://doi.org/10.1016/j.quaint.2019.07.021.

Eger, A., Almond, P.C., Condron, L.M., 2012. Upbuilding pedogenesis under active loess deposition in a super-humid, temperate climate — quantification of deposition rates, soil chemistry and pedogenic thresholds. Geoderma 189–190, 491–501. https://doi.org/10.1016/j.geoderma.2012.06.019.

Evans, M.E., 2001. Magnetoclimatology of aeolian sediments. Geophys. J. Int. 144, 495–497.

Evans, M.E., Heller, F., 1994. Magnetic enhancement and palaeoclimate: study of a loess/palaeosol couplet across the Loess Plateau of China. Geophys. J. Int. 117, 257–264. https://doi.org/10.1111/j.1365-246X.1994.tb03316.x.

Frechen, M., Horváth, E., Gábris, G.y., 1997. Geochronology of middle and upper Pleistocene loess sections in Hungary. Quat. Res. 48, 291–312.

Geiss, C.E., Zanner, C.W., 2007. Sediment magnetic signature of climate in modern loessic soils from the Great Plains. Quat. Int. 162–163, 97–110. https://doi.org/10.1016/j.quaint.2006.10.035.

Geiss, C.E., Egli, R., Zanner, C.W., 2008. Direct estimates of pedogenic magnetite as a tool to reconstruct past climates from buried soils. J. Geophys. Res. Solid Earth 113, 1–15. https://doi.org/10.1029/2008JB005669.

Ghafarpour, A., Khormali, F., Balsam, W., Karimi, A., Ayoubi, S., 2016. Climatic interpretation of loess-paleosol sequences at Mobarakabad and Aghband, Northern Iran. Quaternary Res. 86 (1), 95–109. https://doi.org/10.1016/j.yqres.2016.05.004.

Guérin, G., Mercier, N., Adamiec, G., 2011. Dose-rate conversion factors: update. Ancient TL 29, 5–8.

Halouzka, R., 1966. Základný geologický výskum kvartéru Podunajskej nížiny na Dolnom pohroní a Ipeľskej pahorkatine. Manuscript, GÚDŠ, Bratislava, 9–18. In Slovak.

Hambach, U., 2010. Palaeoclimatic and stratigraphic implications of high resolution magnetic susceptibility logging of Würmian loess at the Krems-Wachtberg Upper-Palaeolithic site. In: Neugebauer-Maresch, C., Owen, L.R. (Eds.), New Aspects of the Central and Eastern European Upper Palaeolithic: Methods, Chronology, Technology and Subsistence. Proceedings of the Prehistoric Commission of the Austrian Academy of Sciences, Vienna, pp. 295e304.

Harden, J.W., 1982. A quantitative index of soil development from field descriptions: Examples from a chronosequence in central California. Geoderma 28, 1–28.

Händel, M., Simon, U., Einwögerer, T., Neugebauer-Maresch, C., 2009a. Loess deposits and the conservation of the archaeological record e the Krems-Wachtberg example. Quat. Int. 198, 46–50.

Händel, M., Simon, U., Einwögerer, T., Neugebauer-Maresch, C., 2009b. New excavations at Krems-Wachtberg e approaching a well-preserved Gravettian settlement site in the middle Danube region. Quartär 56, 187–196.

Heller, F., Shen, C.D., Beer, J., Liu, X.M., Liu, T.S., Bronger, A., Suter, M., Bonani, G., 1993. Quantitative estimates and palaeoclimatic implications of pedogenic ferromagnetic mineral formation in Chinese loess. Earth Planet. Sci. Letters 114, 385–390. https://doi.org/10.1016/0012-821X(93)90038-B.

Hošek, J., Hambach, U., Lisá, L., Grygar, M.T., Horáček, I., Meszner, S., Knésl, I., 2015. An integrated rock-magnetic and geochemical approach to loess/paleosol sequences from Bohemia and Moravia (Czech Republic): Implications for the Upper Pleistocene paleoenvironment in central Europe. Palaeogeogr. Palaeoclimatol. Palaeoecol. 418, 344–358. https://doi.org/10.1016/j.palaeo.2014.11.024.

Hošek, J., Lisá, L., Hambach, U., Petr, L., Vejrostová, L., Bajer, A., Grygar, T.M., Moska, P., Gottvald, Z., Horsák, M., 2017. Middle Pleniglacial pedogenesis on the northwestern edge of the Carpathian basin: A multidisciplinary investigation of the Bíňa pedo-sedimentary section, SW Slovakia. Palaeogeography, Palaeoclimatology, Palaeoecology 487, 321–339. https://doi.org/10.1016/j.palaeo.2017.09.017.

IUSS Working Group WRB, 2015. World Reference Base for Soil Resources 2014, Update 2015 International Soil Classification System for Naming Soils and Creating Legends for Soil Maps. World Soil Resources Reports No. 106. FAO, Rome.

Jary, Z., Ciszek, D., 2013. Late Pleistocene loess-palaeosol sequences in Poland and western Ukraine. Quat. Int. 296, 37–50. https://doi.org/10.1016/j.quaint.2012.07.009.

Jolliffe, I.T., 2002. Principal Component Analysis, second ed. Springer Series in Statistics, p. 405.

Kováč, M. 2000. Geodynamic, paleogeographical and structural evolution of Carpathian - Pannonian region during Miocene: New regard to the Slovak Neogene basins. Veda, Bratislava. 202 p. In Slovak.

Kehl, M., Sarvati, R., Ahmadi, H., Frechen, M., Skowronek, A., 2005. Loess paleosol sequences along a climatic gradient in Northern Iran. Quaternary Sci. J. 55, 151–175.

Kraus, M.J., 1999. Paleosols in clastic sedimentary rocks: their geologic applications. Earth Sci. Rev. 47, 41–70.

Konert, M., Vandenberghe, J., 1997. Comparison of laser grain size analysis with pipette and sieve analysis: a solution for the underestimation of the clay fraction. Sedimentology 44, 523–535.

Long, X., Ji, J., Barr, V., 2016. Climatic thresholds for pedogenic iron oxides under aerobic conditions: Processes and their significance in paleoclimate reconstruction. Quat. Sci. Rev. 150, 264–277. https://doi.org/10.1016/j.quascirev.2016.08.031.

Machette, M.N., 1978. Dating Quaternary faults in the southwestern United States by using buried calcic paleosols. Jour. Research U.S. Geol. Survey 6 (3), 369–381.

Maher, B.A., Alekseev, A., Alekseeva, T., 2002. Variation of soil magnetism across the Russian steppe: Its significance for use of soil magnetism as a palaeorainfall proxy. Quat. Sci. Rev. 21, 1571–1576. https://doi.org/10.1016/S0277-3791(02)00022-7.

Maher, B.A., Alekseev, A., Alekseeva, T., 2003. Magnetic mineralogy of soils across the Russian Steppe: Climatic dependence of pedogenic magnetite formation. Palaeogeogr. Palaeoclimatol. Palaeoecol. 201, 321–341. https://doi.org/10.1016/S0031-0182(03)00618-7.

Maher, B.A., Thompson, R., Zhou, L.P., 1994. Spatial and temporal reconstructions of changes in the Asian palaeomonsoon: a new mineral magnetic approach. Earth Planet. Sci. Lett. 125, 461–471. https://doi.org/10.1016/0012-821X(94)90232-1.

Marriott, S.B., Wright, V.P., 1993. Paleosols as indicators of geomorphic stability in two Old Red Sandstone alluvial suites. South Wales. J. Geol. Soc. London 150, 1109–1120.

Marković, S.B., Stevens, T., Kukla, G.J., Hambach, U., Fitzsimmons, K.E., Gibbard, P., Buggle, B., Zech, M., Guo, Z., Hao, Q., Wu, H., O'Hara Dhand, K., Smalley, I., Újvári, G., Sümegi, P., Timar-Gabor, A., Veres, D., Sirocko, F., Vasiljević, D.A., Jary, Z., Svensson, A., Jović, V., Lehmkuhl, F., Kovács, J., Svirčev, Z., 2015. Danube loess stratigraphy — towards a pan-European loess stratigraphic model. Earth Sci. Rev. 148, 228–258. https://doi.org/10.1016/j.earscirev.2015.06.005.

Mazúrová, V. 1978. Terasy riek čs. Karpát a ich vzťah k terasám Dunaja. Geografický časopis, 30, 4, 281–301. In Slovak.

Minaříková, D., 1969. Petrografie kvartérních sedimentů v údolí Dunaje mezi Komárnem a Štúrovem. Geologické práce, Správy, 49, 193–214. In Czech.

Motavalli-Anbaran, S.-H., Zeyen, H., Brunet, M.-F., Ardestani, V.E., 2011. Crustal and lithospheric structure of the Alborz Mountains, Iran, and surrounding areas from integrated geophysical modeling. Tectonics 30, TC5012. https://doi.org/10.1029/2011TC002934.

Morrison, R.B., 1978. Quaternary soil stratigraphy—concepts, methods, and problems. In: Mahaney, W.C. (Ed.), Quaternary Soils. Geo Abstracts, Norwich, pp. 77–108.

Mush, D.R. 2007a. Loess deposit, origins and properties. In: Elias, S.A. (ed.) Encyclopedia of Quaternary Science, ELSEVIER, pp. 1405-1418.

Muhs, D.R. 2007b. Paleosols and wind-blown sediments. In: Elias, S.A. (Ed.) Encyclopedia of Quaternary Science, pp. 2075-2086. DOI: 10.1016/B0-44-452747-8/00378-1.

Muhs, D.R., and Bettis, E.A., III, 2003. Quaternary loess-paleosol sequences as examples of climate-driven sedimentary extremes, in: Chan, M.A., and Archer, A.W., (Eds.) Extreme depositional environments: Mega end members in geologic time: Boulder, Colorado, Geological Society of America Special Paper 370, pp. 53–74.

Muhs, D.R., McGeehin, J.P., Beann, J., Fisher, E., 2004. Holocene loess deposition and soil formation as competing processes, Matanuska Valley, southern Alaska. Quat. Res. 61, 265–276.

Muhs, D.R., Budahn, J.R., Skipp, G.L., McGeehin, J.P., 2016. Geochemical evidence for seasonal controls on the transportation of Holocene loess, Matanuska Valley, southern Alaska, USA. Aeol. Res. 21, 61–73.

Murray, A.S., Wintle, A.G., 2003. The single aliquot regenerative dose protocol: potential for improvements in reliability. Radiat. Meas. 37, 377–381.

Novothny, Á., Horváth, E., Frechen, M., 2002. The loess profile at Albertirsa, Hungary - improvements in loess stratigraphy by luminescence dating. Quat. Int. 95–96, 155–163.

Novothny, Á., Frechen, M., Horváth, E., Bradák, B., Oches, E.A., McCoy, W.D., Stevens, T., 2009. Luminescence and amino acid racemization chronology of the loess-paleosol sequence at Süttő, Hungary. Quat. Int. 198, 62–76.

Novothny, Á., Frechen, M., Horváth, E., Wacha, L., Rolf, C., 2011. Investigating the penultimate and last glacial cycles of the Süttő loess section (Hungary) using luminescence dating, high-resolution grain size, and magnetic susceptibility data. Quat. Int. 234, 75–85.

Novothny, Á., Barta, G., Végh, T., Bradák, B., Surányi, G., Horváth, E., 2019. Correlation of drilling cores and the Paks brickyard key section at the area of Paks, Hungary. Quaternary International, in press.

Novothny, Á., Kiss, B., Sági, T., Bradák, B., Oches, E.A., McCoy, W.D., Thiel, C., Surányi, G., Végh, T., Szeberényi, J., Csonka, D., Barta, G., Kaufman, D., Ntaflos, T., Horváth, E. Dating and petrographic investigation of loess-paleosol sequences containing the Bag Tephra from the Northern-Carpathian Basin – Can the Bag Tephra be used as a marker horizon? - in prep.

Prescott, J.R., Hutton, J.T., 1994. Cosmic ray contribution to dose rates for luminescence and ESR dating: large depth and long-term time variations. Radiat. Meas. 23, 497–500.

Prins, M.A., Vriend, M., Nugteren, G., Vandenberghe, J., Lu, H., Zheng, H., Weltje, G.J., 2007. Late Quaternary aeolian input variability on the Chinese Loess Plateau: inferences from unmixing of loess grain-size records. Quat. Sci. Rev. 26, 230–242.

Rees-Jones, J., 1995. Optical dating of young sediments using fine-grain quartz. Ancient TL 13, 9–14.

Rosenthal, G., Rosenthal, J., 2011. Statistics and Data Interpretation for Social Work. Springer Publishing Company, p. 512 p..

Schmidt, Z., 1968: Fossil mollusca fauna of sediment complex at Buci (Danube valley), Svodín (Hron valley) and Dolinka (Ipel valley). Manuscript, archív Geofondu, ŠGÚDŠ, Bratislava.- in Slovak.

J. Seneš 1971. Korrelation des Miozäns der Zentralen Paratethys (Stand, 1970). Geologický Zborník, 22, 1 1970 SAV Bratislava 3 9.

Shaetzl, R., Anderson, S., 2005. Soils - Genesis and Geomorphology. Cambridge University Press, p. 817 p..

Smalley, I., O'Hara-Dhand, K., Wint, J., Machalett, B., Jary, Z., Jefferson, I., 2009. Rivers and loess: the significance of long river transportation in the complex event sequence approach to loess deposit formation. Quat. Int. 198, 7–18.

Stevens, T., Marković, S.B., Zech, M., Hambach, U., Sümegi, P., 2011. Dust deposition and climate in the Carpathian Basin over an independently dated last glacial–interglacial cycle. Quat. Sci. Rev. 30, 662–681.

Szeberényi, J., Kovács, J., Bradák, B., Barta, G., Csonka, D., Medveďová, A., Rostinsky, P., Kiss, K., Varga, Gy,2020. Experiencing new perspectives in the application of reflectance spectroscopy in loess research. Quaternary International In press (2020). DOI: 10.1016/j.quaint.2019.09.035.

Szeberényi, J., Józsa, S., Simon, I., Kiss, K., Bradák, B., Viczián, I., 2015. An examination of the pebbly sediments of the Visegrád Gorge area, with special attention to their significance for the division of the morphostratigraphy of the Danube terrace systems (in Hungarian). Földtani Közlöny 145 (4), 367–383.

Terhorst, B., Kühn, P., Damm, B., Hambach, U., Meyer-Heintze, S., Sedov, S., 2014. Paleoenvironmental fluctuations as recorded in the loess-paleosol sequence of the Upper Paleolithic site Krems-Wachtberg. Quat. Int. 351, 67–82. https://doi.org/10.1016/j.quaint.2013.03.045.

Terhorst, B., Sedov, S., Sprafke, T., Peticzka, R., Meyer-Heintze, S., Kühn, P., Solleiro Rebolledo, E. 2015. Austrian MIS 3/2 loess–palaeosol records—Key sites along a west–east transect. Quaternary International 351, 67-82. https://www.sciencedirect.com/science/article/abs/pii/S0031018214005318.

Thiel, C., Buylaert, J.-P., Murray, A., Terhorst, B., Hofer, I., Tsukamoto, S., Frechen, M., 2011. Luminescence dating of the Stratzing loess profile (Austria) - testing the potential of an elevated temperature post-IR IRSL protocol. Quat. Int. 234, 23–31.

Újvári, G., Molnár, M., Novothny, Á., Páll-Gergely, B., Kovács, J., Várhegyi, A., 2014a. AMS 14C and OSL/IRSL dating of the Dunaszekcső loess sequence (Hungary): chronology for 20 to 150 ka and implications for establishing reliable age–depth models for the last 40 ka. Quat. Sci. Rev. 106, 140–154.

Újvári, G., Varga, A., Raucsik, B., Kovács, J., 2014b. The Paks loess-paleosol sequence: a record of chemical weathering and provenance for the last 800 ka in the mid-Carpathian Basin. Quat. Int. 319, 22–37.

Újvári, G., Kele, S., Bernasconi, S.M., Haszpra, L., Novothny, Á., Bradák, B., 2019. Clumped isotope paleotemperatures from MIS 5 soil carbonates in southern Hungary. Palaeogeogr. Palaeoclimatol. Palaeoecol. 518, 72–81. https://doi.org/10.1016/j.palaeo.2019.01.002.

Vandenberghe, J., 2013. Grain size of fine-grained windblown sediment: A powerful proxy for process identification. Earth Sci. Rev. 121, 18–30. https://doi.org/10.1016/j.earscirev.2013.03.001.

Vandenberghe, J., Zhisheng, A., Nugteren, N., Huayu, L., Van Huissteden, K., 1997. New absolute time scale for the Quaternary climate in the Chinese loess region by grain-size analysis. Geology 25 (1), 35–38.

Varga, Gy, Cserháti, Cs, Kovács, J., Szalai, Z., 2016. Saharan dust deposition in the Carpathian Basin and its possible effects on interglacial soil formation. Aeolian Res. 22, 1–12.

Vass, D., 2002. Lithostratigraphy of Western Carpathians: Neogene and Buda Paleogene. GÚDŠ, Bratislava, p. 202.

Verosub, K.L., Fine, P., Singer, M.J., TenPas, J., 1993. Pedogenesis and paleoclimate: Interpretation of the magnetic susceptibility record of Chinese loess-paleosol sequences. Geology 21, 1011–1014.

Vriend, M., Prins, M.A., 2005. Calibration of modelled mixing patterns in loess grainsize distributions: an example from the north-eastern margin of the Tibetan Plateau, China. Sedimentology 52 (1361), 1374.

Wacha, L., Rolf, C., Frechen, M., Hambach, U., Galović, L., Duchoslav, M., 2018. The Last Glacial aeolian record of the island of Susak (Croatia) as seen from a high-resolution grain-size, rock and palaeo-magnetic analysis. Quat. Int. 494, 211–224.

Wintle, A.G., 1973. Anomalous fading of thermoluminescence in mineral samples. Nature 245, 143–144.

Wright, V.P., Marriott, S.B., 1996. A quantitative approach to soil occurrence in alluvial deposits and its application to the Old Red Sandstone of Britain. J. Geol. Soc. London 153, 907–913.

Yi, S., Buylaert, J.-P., Murray, A.S., Lu, H., Thiel, C., Zeng, L., 2016. A detailed post-IR IRSL dating study of the Niuyangzigou loess site in northeastern China. Boreas 45, 644–657.

Zech, R., Zech, M., Marković, S., Hambach, U., Huang, Y., 2013. Humid glacials, arid interglacials? Critical thoughts on pedogenesis and paleoclimate based on multi-proxy analyses of the loess–paleosol sequence Crvenka, Northern Serbia. Palaeogeogr. Palaeoclimatol. Palaeoecol. 387, 165–175. https://doi.org/10.1016/j.palaeo.2013.07.023.

Zhao, J.-B., Ma, Y.-D., Cao, J.-J., Hao, Y.-F., Shao, T.-J., Liu, X.-M., 2020. Holocene pedostratigraphic records from the southern Chinese Loess Plateau and their implications for the effects of climate on human civilization. Catena 187 (2020), 104410. https://doi.org/10.1016/j.catena.2019.104410.